VISION BASED TARGET TRACKING GUN TURRET

A dissertation submitted to the
Department of Electrical Engineering, University of Moratuwa
in partial fulfillment of the requirements for the
Degree of Master of Science

by
WANNIACHCHIGE INDU DILSHAN ABEYW ARDENA

Supervised by: Dr. Rohan Munasinghe

Department of Electrical Engineering
University of Moratuwa
Sri Lanka

2010

94544

Abstract

This project explores the task of tracking a moving target (aircraft) and pointing an anti aircraft gun perched on a pan tilt base in a real time combat environment. The purpose of this process is to study the dynamics of the mechanism, controlling requirements, software requirements and subsystems requirements needed for the implementation of a commercially viable air defense system. A laboratory model is developed to represent the pan-tilt gun turret, dynamically analyzed, controllers designed and field testing carried out. Though the system is designed as a laboratory model, every attempt is made to reach the level of sophistication and detail required for a military grade target tracking system. The thesis formulates a clearly identifiable procedures and steps which need to be carried out in the implementation of such a system. Due to the obvious unavailability of target tracking data from a radar system, target position information from machine vision software is used. The scope of the project is limited to; designing the interface between Camera, CPU and servo-controllers, designing the mounting base for the artillery with the pan-tilt mechanism, Modeling the plant and designing the ,controller.

Field testing reveals the validity of the procedures mentioned above and the satisfactory results obtained through such procedure.

DECLARATION

The work submitted in this dissertation is the result of my own investigation, except where otherwise stated.

It has not already been accepted for any degree, and is also not being concurrently submitted for any other degree.

UOM Verified Signature

Dilshan Abeywardena
08/02/2010

I endorse the declaration by the candidate.

UOM Verified Signature

Dr Rohan Munasinghe

CONTENTS

Acknowledgement

Thanks are due first to my supervisor, Dr Rohan Munasinghe, for his great insights, perspectives and guidance. My sincere thanks go to the officers in the Post Graduate Office, Faculty of Engineering, University of Moratuwa, Sri Lanka for helping in various ways to clarify the things related to my academic works in time with excellent cooperation and guidance. Sincere gratitude is also extended to the officers who serve in the Department of Electrical Engineering office.

The author extends sincere gratitude to Professor Lanka Udawatta and Dr. Chandima Dedduwa Pathirana for their untiring efforts in coordinating the MSc in Industrial automation program and encouraging words in every step of the way of the above program.
The author had to make many visits to the local machinist in the process of designing and building the pan-tilt base and was pleasantly surprised by the skill and aptitude of these experienced craftmen. The design process was a marriage between mechanical engineering and electronics engineering among other disciplines, To this end, I may not have been able to finish off the mechanism if not for valuable suggestions from workers at the local machinist shop.

Lastly, I should thank my family for their understanding and perseverance during the last two years, friends and colleagues who have not been mentioned here personally in making this educational process a success. I could not have made it without your supports.

List of Figures

List of Tables

Chapter 1

Introduction

1.1 Target Tracking Fundamentals

Tracking a target involves the knowing the whereabouts of an object at all times. In order to do this, tracking systems make use of various features of the target being tracked, such as, its image, radar cross section, mass of the object etc.
Target tracking has many fields of application, in the military field target tracking plays a major role in automated missile guidance systems and anti aircraft artillery batteries. In the field of industrial automation, target tracking is extensively used in automatic guided vehicles (AGV). Tracking mechanism may contain single or multiple sensors. In case of multiple sensors, data fusion should be applied to make use of most suitable data from each sensor.

The challenges that need to be over come during target tracking are numerous, the size of the target its speed, material, color, shape, background condition, the distance from the tracking sensor, and the quality of the sensors them selves influence performance.

The target may be large and easily identifiable against a contrasting background or it may be small and blend in to the background making it difficult to distinguish between the noise and the actual target.

Every sensor has a sensing delay, In case of primary radar systems the target is sensed once every rotation of the radar antenna. therefore between two sensing cycles the whereabouts of the target is not known therefore if the target is a fast moving one, compared to the sensor cycle time, data gathered from this sensor(radar) may not be too useful in tracking the particular target.
In case of a camera, ultra sound sensors, infrared sensors, thermal sensors the delay is due largely to the A to D conversion process.

Modern military technologies have developed various materials that absorb radar waves making the radar cross section of certain targets very small furthermore the target is shaped in such a way that it reflects the least amount of radar energy back to the sensors making radar detection even more difficult.

Condition's in which the tracking system has to operate does not stay static. Whether conditions, lighting conditions influence target tracking.
Last but now least, the quality of the sensors them selves affect target tracking.
All above examples compound to produce a very noisy sensor output.

Following publications are more relevant to this project among existing work on related subjects,
Stanciu, Paul Y Oh (2002) studied visually servoed tracking to augment camera tele-operators. Where they designed control systems to keep the target positioned at the center of the image automatically augmenting the camera operators inputs.

Bharat N. Shah, Paul Y Oh (2002) studied biometric visual servoing using a partitioned control scheme. This study presented a partitioned controller for the visually servoed tracking of objects using both image and kinematics data. Resulting design showed similar performance to vision systems in biology.

Sisil Kumarawadu, Kiego Watanabe (2007) studied high performance Object tracking and fixation using a robotic head with stereo vision.

1.2 Motivation

Motivation for the project was born out of the unique control systems challenge presented by the process of target tracking. This project runs through the entire gamut of topics covered during the Post Graduate Diploma stage. The writer acknowledges that project was not under taken to solve a particular immediate problem but to gain experience and develop Procedures using existing technologies to solve the much complex problem of a military grade low level anti-aircraft artillery system, capable of engaging fixed wing aircraft, helicopters and unmanned aerial vehicles(UAV). Hence the scaled down laboratory model of the life size system. Further more there are several impediments in developing a full scale version. Such as funding and regulatory restrictions being a military application.

Srilanka, being an island nation will have to guard it self against airborne enemies in the future. We have seen in the past that our defenses are most vulnerable to airborne attacks of any nature. Our enemies need not acquire highly sophisticated aircraft to threaten the very heart of Sri Lanka. Therefore it is prudent to build up our air defenses for such attacks in the future. In this Endeavour countries like ours face the formidable obstacle of foreign exchange out flow in the form of defense expenditure. Air defense systems cost large amounts of money which we can ill afford. Therefore, it is unwise not to consider a system of our own, especially given the fact that the technology required is more or less available and accessible (alas in fragmented form). Further more, if such a system could be developed, it could be commercialized to bring in valuable foreign exchange in the future. Though such systems are available in the military hardware market, such as the Russian ZSU-23/4 (Shilka) 23mm quad automatic Self Propelled Anti-Aircraft (SPAA) gun, rarely does the technology made available freely in the form of blue prints as such each country needs to develop its own culture of military hardware technology.

1.3 Goals and Achievements

The main goal of this project is to develop the technologies required for the full scale target tracking AAA system of a complex air defense system and to implement a scaled down prototype. To this end the designer seeks to develop clearly identifiable procedures for the purpose of;

- System modeling techniques
- Control systems;
- Motor Drivers and Electronics
- System implementation using embedded systems for real time control
- Target characteristics analysis etc.

In order to achieve aforementioned goals, we needed a pan-tilt base which is capable of performing as a laboratory model for the life size system and displays the dynamic characteristics of a life size system. Therefore the laboratory model need to be fairly large enough such that it incorporates all the mechanical characteristics associated with a real systems and in significant quantities, i.e: coupling effects, carioles force, friction, gravity etc. Therefore the development of such a system is one of the primary goals of the project.

Following milestones in relation to the goals stated above have been achieved.

- A fully functional pan tilt mechanism
- A servo controller having two analog inputs two digital inputs and two analog outputs (PWM)
    - Servo controller is capable of driving 8 amperes to two motors at 24 V DC
    - Servo controller is capable of In Circuit Serial Programming
- A machine vision system for target identification.
- Interface between Target tracking system and Pan tilt platform.
- Simulink model of the system
- Solid works model for calculating inertia values
- Bode analysis of the Pan-Tilt platform
- Target characteristics using Fast Fourier Transformation techniques
- Field test of vision based target tracking system.
- Through above achievements, the author was able to confirm that the design procedure is valid and can yield usable results.

Chapter 2

Target Identification and Tracking Techniques

Any designer is spoilt for choice when it comes to technologies available for identifying a target. Prominent among them are; Radar, infrared imaging, thermal imaging, vision and ultra sound etc. When it comes to identifying a target at long distances most of these choices fail to achieve reliable results, for instance, infrared imaging, thermal imaging and vision all require the target to be within line of sight from the tracking camera. Furthermore these tracking cameras struggle to pick up anything beyond 500 meters. Therefore it only leaves one candidate to track long distance targets i.e; Radar.

Commercial aviation is uses a technology called "secondary surveillance radar" or (SSR). This system tracks the target by locking on to a beacon sent out by the aircraft being tracked. But it is obvious that we cannot put beacons on an enemy aircraft. Therefore military aviation is has to work with primary radar.

The proposed system uses a remote primary radar unit for target tracking and identification; however at this stage of development the author is unable to acquire target information from a real radar system. Therefor a computer vision system capable of delivering target information similar to that of primary radar is used. This computer vision system feeds pan and tilt angle data to the turret system. Some kind of intelligent system or a human interface is required between the tracking system and the gun turret to identify friend or foe. However, design of such a system is not covered within this project. In summary the complete system consists of 1.computer vision system for laboratory model, 2. Intelligent friend or foe identification system, 3. Gun turret. At this point it is prudent to point out that the system is a closed loop system, With any closed loop system, the bandwidth of the system is determined by the slowest component in the loop. In this case it is the radar detection system.

2.1 System overview

The system is consisted of a tracking system, intelligent friend of foe identification system and the pan-tilt anti aircraft gun turret.
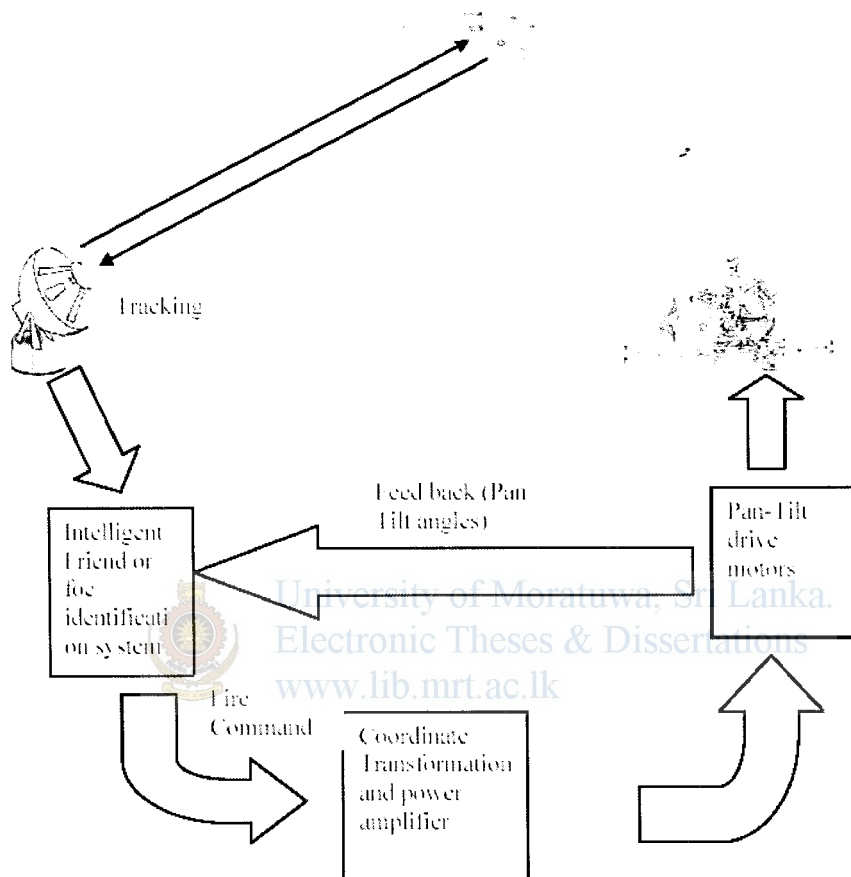
Fig 2.1 Automated target tracking air defense system

2.2 Control Technologies

There are several ways by which the pan-tilt base can respond to the error between the desired angle and the actual angle. It can switch ON or OFF the motor in either direction depending on whether the error is positive or negative. This is called simple ON/OFF control otherwise it can produce a control signal which is proportional to the error this is proportional (P) control.

If it produces a control signal proportional to the rate of change of the error it is called Derivative (D) control. It can also produce a control signal which is proportional to the integral of the error with time and this is integral (I) control. The controller can also use combinations of P, I or D control. However other options available to the designer are partitioned PD control, adaptive control, computed torque control and inversion based control [6], [7], [8], all of which has demonstrated better control performance over PID control. However following section examines advantages and disadvantages of using each type of control technology to arrive at the most appropriate type of control technology for the system.

Fig. 2.2 System Model
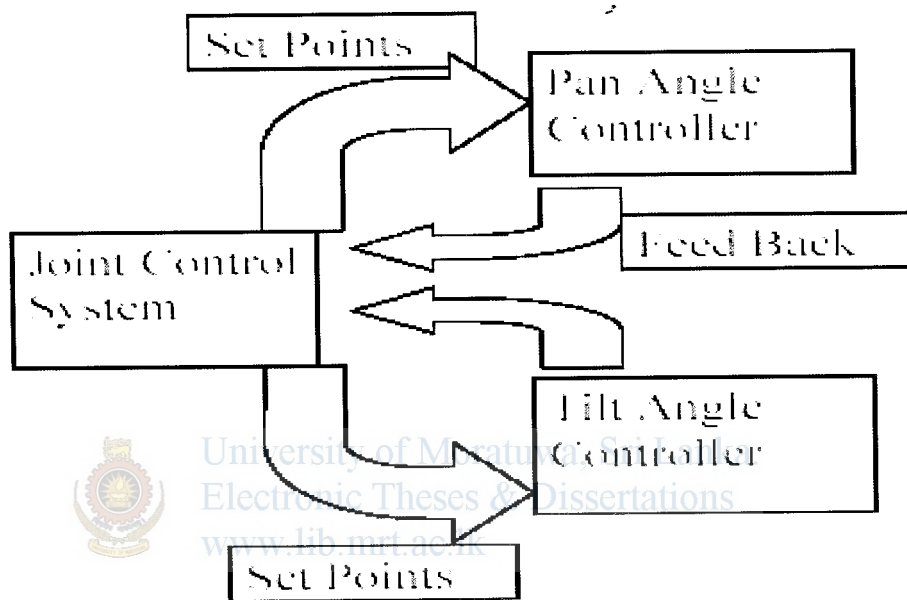
It is clear that our system is a multi input multi output system (MIMO). to simplify the problem each joint(Pan and tilt) is considered separately and assumed to be independent. There fore we covert the above MIMO system in to two Single input single output systems(SISO). Control schemes considered for this system include, PID control or proportional Integral and derivative control.

In PID control, all non-linear effects are considered as noise. PID control scheme has the unique capability of overcoming all such noise inputs, given adequate bandwidth is available with the system. Therefore the ultimate justification for use of PID control scheme is dependent on the final out come of the system, i.e, if the system is capable of achieving specified performance benchmarks, use of PID controller is justified.

The use of linear control schemes is only valid for those systems whose behavior can be mathematically modeled by linear differential equations [6]. Linear control techniques for manipulator control are essentially an approximate method and for this a manipulator joint should be modeled as a linear second-order system.

2.3 Linear Second Order SISO Model of a Manipulator Joint.

Pan and tilt joints of the mechanism is considered as a manipulator joint and linear second order model is given below [6]
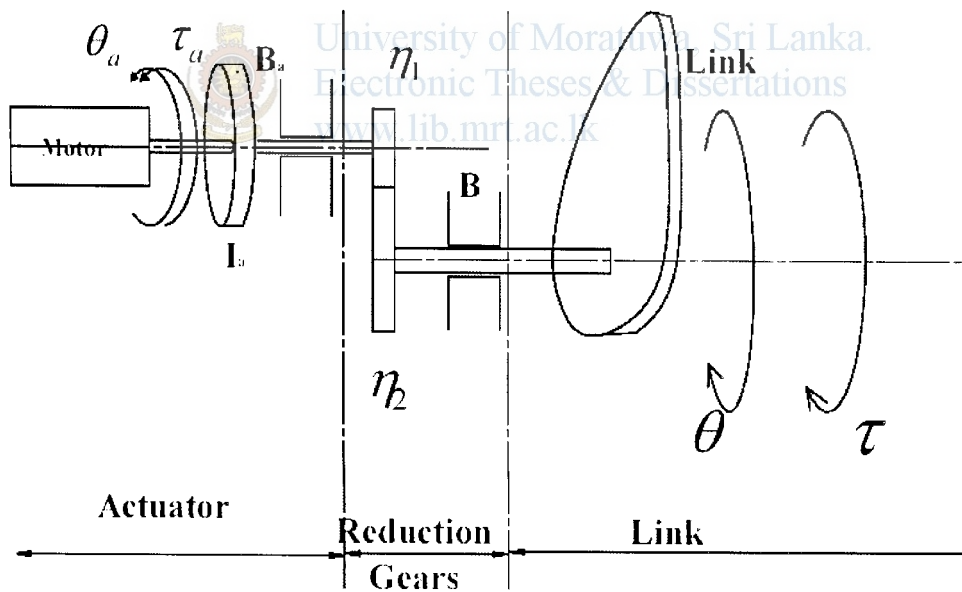

Fig 2.3 Linear second order SISO model of a manipulator joint

$$\eta = \frac{number\ of\ teeth\ on\ the\ gear\ of\ link\ shaft}{number\ of\ teeth\ on\ the\ gear\ of\ actuator\ shaft} = \frac{\eta_1}{\eta_2} \qquad (2.1)$$

The gear ration η is greater than 1 for a reduction gear. The gear

$$\tau = \eta\tau_a \qquad (2.2)$$

$$\theta = \frac{1}{\eta}\theta_a \tag{2.3}$$
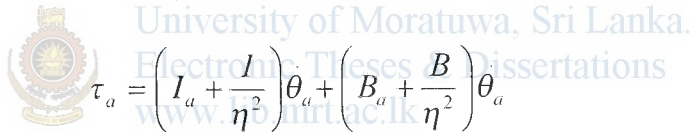
$$\theta = \frac{1}{\eta}\dot{\theta}_a \tag{2.4}$$

The link torque τ when reflected to the actuator side, is scaled down by a factor of η, the gear ratio. I_a is the inertial of rotor of the actuator and B_a is the viscous friction coefficient at actuator bearings, for the rotational mass-damper system, the torque required at the actuator shaft is given by

$$\tau_a = I_a\ddot{\theta}_a + B_a\dot{\theta}_a + \frac{\tau}{\eta} \tag{2.5}$$

$$\tau_a = I_a\ddot{\theta}_a + B_a\dot{\theta}_a + \frac{1}{\eta}(I\ddot{\theta} + B\dot{\theta}) \tag{2.6}$$

Where I_a is the inertia of the load and B is the viscous friction coefficient for the load.

In terms of actuator variables,

$$\tau_a = \left(I_a + \frac{I}{\eta^2}\right)\ddot{\theta}_a + \left(B_a + \frac{B}{\eta^2}\right)\dot{\theta}_a \tag{2.7}$$

In terms of link variables,

$$\tau = \left(I + \eta^2 I_a\right)\ddot{\theta} + \left(B + \eta^2 B_a\right)\dot{\theta} \tag{2.8}$$

The link torque τ is obtained from the dynamic model of the joint.

The dynamic equation of a joint I of a manipulator is given by;

$$\tau_i = \sum_j M_{ij}\ddot{q}_j + \sum_j\sum_k h_{ijk}\dot{q}_j\dot{q}_k + G_i \tag{2.9}$$

Eq (2.9) equation is rewritten below with the subscript i for joint i dropped for convenience.

$$\tau = \sum_j M_j\ddot{\theta}_j + \sum_j\sum_k h_{jk}\dot{\theta}_j\dot{\theta}_k + G \tag{2.10}$$

Where G is the Gravity term and only comes into effect when motion is against gravity.
Note that the equation does not include the effects of friction, backlash and elastic deformations.

The viscous friction is directly proportional to the velocity and can be included in the model.

$$\tau = \sum_j M_j \, \ddot{\theta}_j + \sum_j \sum_k h_{ijk} \, \dot{\theta}_j \, \dot{\theta}_k + B\dot{\theta} + G \qquad (2.11)$$

Where B is the viscous friction coefficient at the link bearings.
The terms in above equation are split into linear decoupled and non linear interacting terms. The two linear decoupled terms are $M\ddot{\theta}$ from the first summation term and the third term $B\dot{\theta}$. The remaining terms are non linear interacting terms and are grouped together and denoted as 'd' that is

$$d = \sum_{\substack{j=1 \\ j \neq i}}^{n} M_j \, \ddot{\theta}_j + \sum_j \sum_k h_{jk} \, \dot{\theta}_j \, \dot{\theta}_k + G \qquad (2.12)$$

Equation 2.11 is written as;

$$\tau = M\ddot{\theta} + B\dot{\theta} + d \qquad (2.13)$$

Substituting τ from Eq. (2.10) in to Eq. (2.5) and rearranging, the actuator torque is obtained as;

$$\tau_a = \left(I_a + \frac{M}{\eta^2} \right) \ddot{\theta}_a + \left(B_a + \frac{B}{\eta^2} \right) \dot{\theta}_a + \frac{d}{\eta} \qquad (2.14)$$

Since the pan tilt mechanism is highly geared, $\eta = 80$ for pan mechanism and $\eta = 66$ for tilt mechanism it is reasonable to ignore the contribution of the non linear interacting term d and still guarantee a good trajectory-tracking performance.
Neglecting nonlinear terms, the actuator torque reduces to;

$$\tau_a = I_{eff} \, \ddot{\theta}_a + B_{eff} \, \dot{\theta}_a \qquad (2.15)$$

Where I_{eff} is the effective inertia and B_{eff} is the effective damping with ;

$$I_{eff} = I_a + \frac{M}{\eta^2} \qquad (2.16)$$

$$B_{eff} = B_a + \frac{B}{\eta^2} \qquad (2.17)$$

Load torque can be written as;

$$\tau = I_{eff}\, \ddot{\theta} + B_{eff}\, \dot{\theta} \tag{2.18}$$

Since the configuration dependent term 'M' is reduced by a factor η^2, with $\eta \gg 1$, I_{eff} is almost constant for highly geared manipulators.

Therefore the inertia term seen by the system is effectively the inertia term of the armature I_a.
And we will have to obtain B_{eff} using experimental methods.

2.4 Motor model
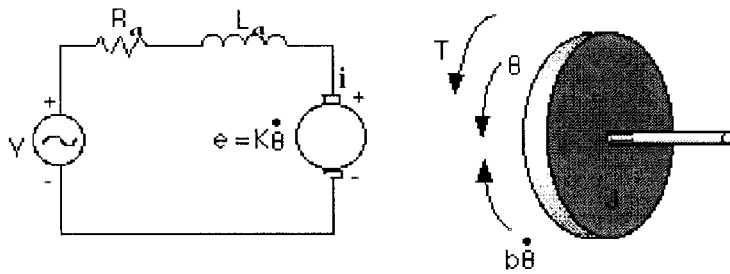
Fig 2.5 motor model

$$L_a \frac{di_a}{dt} + R_a i_a = v - K_e\, \dot{\theta}_a \tag{2.19}$$

$$e = K_e \dot{\theta}_a \tag{2.20}$$

An inertial load τ is connected to the motor armature via a gearbox with ratio η. The configuration is illustrated in fig 2.5

$$\tau = I_{eff}\, \ddot{\theta} + B_{eff}\, \dot{\theta} \quad \text{(From 2.18)} \tag{2.21}$$

$$\tau_a = K_e i_a \tag{2.22}$$

Above equations can be used to construct a signal flow graph of the electric motor/load which can be realized in SIMULINK.

Implementation of Vision Based Target Tracking System

Implementation consists of design and construction of the Turret base and integrating it with the machine vision system

3.1 Design and Construction of Turret Base
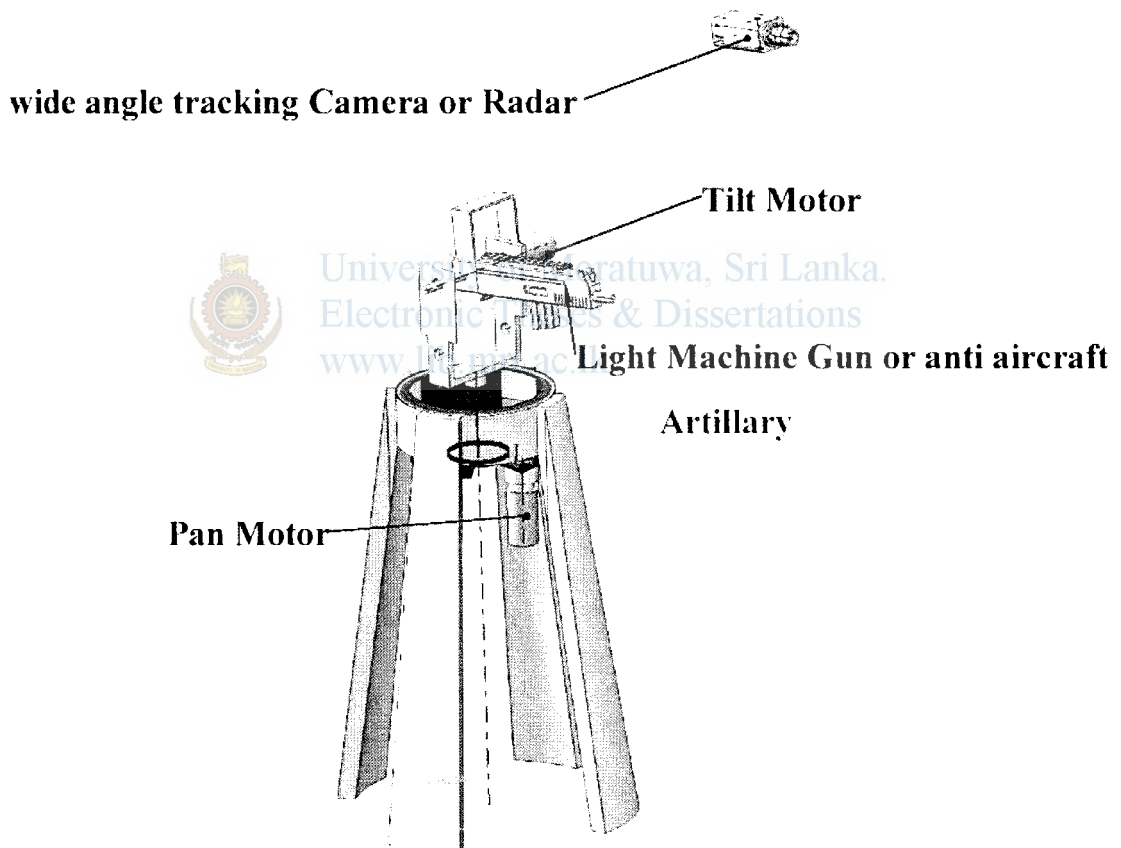
Fig 3.1 Solidworks impression of the final Gun turret system (laboratory model)

Fig 3.1 shows the envisioned gun turret system (laboratory model). According to Hutchinson (1996) this configuration can be considered as a fixed camera configuration. Wide angle camera is displayed which is used in the laboratory model in place of the radar system. AAA is replaced on the model with a light machine gun (LMG). Entire system is mounted on a metal stand which is of 3 feet in height. The camera is situated at a distance from the gun turret and does not have any mechanical link with the base.

3.1.1 Rotation Base

Rotation base of the system is a commercially available base constructed around stainless steel shaft of 12 mm in diameter. The rotating part of the mechanism rotates around this stationary shaft supported by two roller bearings. Mounting for the whole mechanism is attached to the stationary Stainless Steel shaft from the bottom of the mechanism.
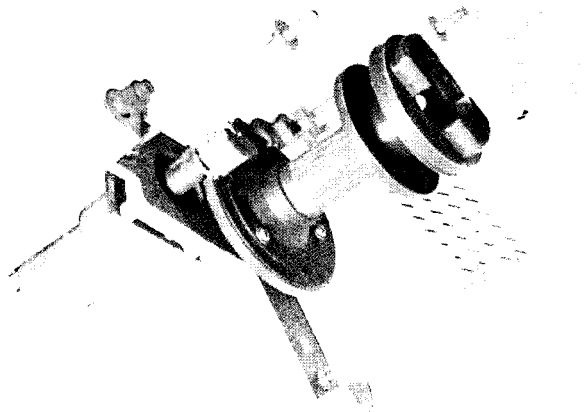
Fig 3.2 Rotation base

The base came with a 2 pole stepper motor as the actuator, which was replaced by the selected DC motor to achieve higher torque and to simplify driver electronics design.
The actuator is connected to the base via a gear wheel system with a gears ratio of 12. The motor it self has a gear box with a 5.9:1 gears ratio, which gives an overall gears ratio of 70.8:1.
My contribution to this base is,
- Replacing the stepper motor a PM DC motor.
- Designing the mounting plate between the base and the DC motor
- Designing the mounting plate for the pan angle sensor.
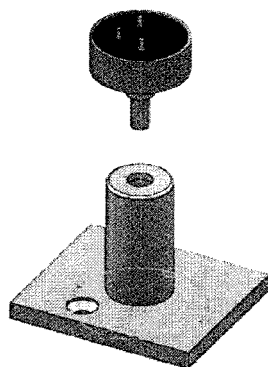
Fig3.3   fixing plate for the sensor potentiometer
- Attaching the 10 turn 10k potentiometer (pan angle sensor) to the motor shaft.

3.1.2 Tilt Base

Tilt base was designed from scratch by the author. It consists of a tilt Frame to which tilt motor, Gear box and the payload (Gun or Anti aircraft artillery) is connected. It is made out of steel and weighs approximately 7.8 kg
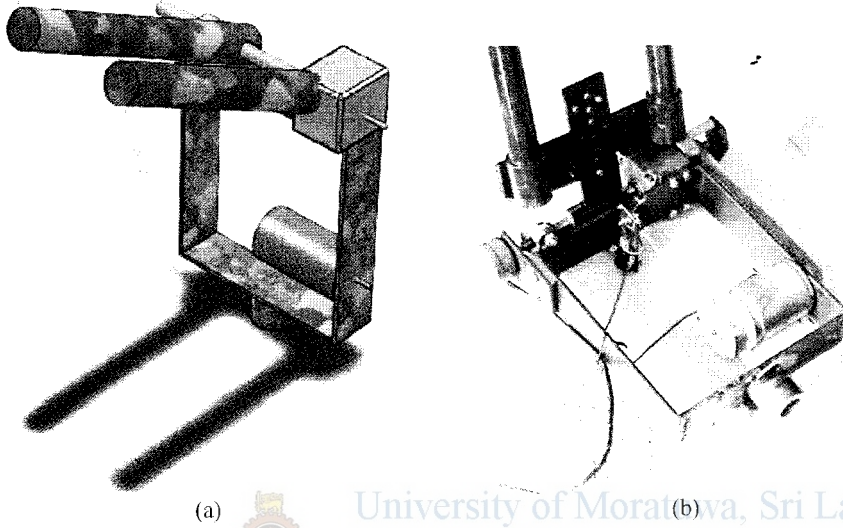
(a)   (b)

Fig 3.4(a) tilt base solid works model, 3.4(b) tilt base after construction

3.1.3 Mounting Plate

Mounting plate is a heavy steel plate with a bearing guide, for the pan rotation. It acts as the mounting plate and as a stabilizing guide for pan rotation. It is made with heavy gage steel to give more stability to the mechanism
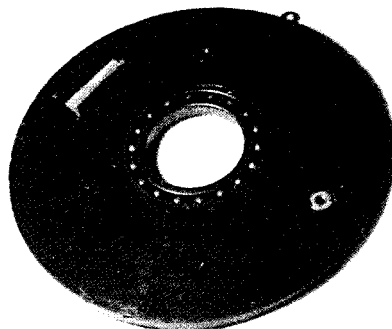
Fig 3.5 Mounting plate

3.1.4 Tilt Movement Gear Box.

Tilt movement gear box is a commercially available gear box (procured from ebay) with a turns ration of 20:1
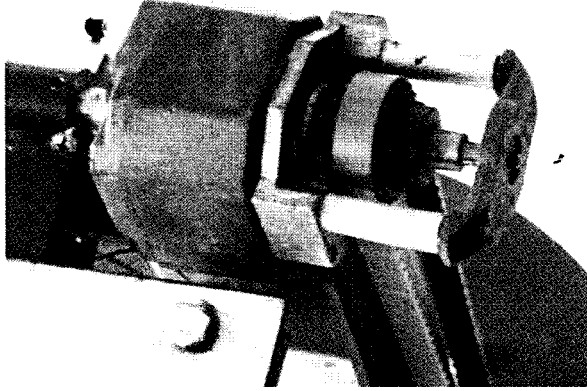
Fig 3.6 Tilt movement gear box with 20:1 gears ratio

3.1.5 Complete System
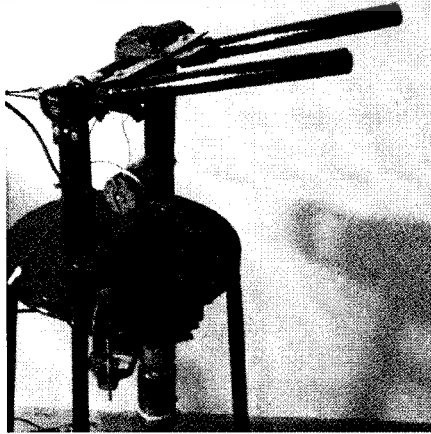
Fig 3.7 shows the final product after mounting on a pedestal.

3.1.6 Design Specifications

Bandwidth of the system (from Chapter 4)

Pan mechanism Position loop $= 2\pi$ rad/s
Pan mechanism Velocity loop $= 141.6$ rad/s

Tilt mechanism position loop $= 2\pi$ rad/s
Tilt mechanism velocity loop $= 155$ rad/s

3.1.7 Selection of Motors

Selection of motors is an exercise of selecting the best out of available limited options;
Since the tilt mechanism needs to operate against gravity it needs a higher torque motor than the pan motor, therefore following motors are selected for the pan and tilt mechanisms respectively.

Pan motor:

Manufacturer:	Pittman
Operating voltage:	24V
Power:	18W
Peak Current	5 A
Maximum rotational speed	2600 rpm
Armature resistance	6.1 Ohm
Torque:	0.33Nm
Armature inductance:	4.6 mH
Rotor inertia:	0.00019 kg/m^2

Tilt motor:

Manufacturer:	Toshhiba
Operating voltage:	24V
Power	50W
Peak Current	8 A
Maximum rotational speed	2600 rpm
Armature resistance	2.4 Ohm
Torque	0.99 Nm
Armature inductance	2.08 mH
Rotor inertia	

3.1.8 Selection of Sensors

Since the selected motors did not come with built in tachometers or angular sensors, several types of sensors were considered at the initial stage.

      a. Quadrature encoders
      b. Absolute digital encoders
      c. Incremental encoders
      d. Simple potentiometers
      e. Absolute analog encoders (contact less type)
      f. Absolute analog encoders (contact type)

Following criteria were considered when selecting sensors

- Resolution
- Conversion speed (in case of A to D conversion)
- Requirement of complex electronic circuits for filtering/decoding etc
- Mechanical resistance imposed on the system.
- Temperature sensitivity
- linearity
- Cost

a. Quadrature encoder: (Appendix F)

Quadrature encoders available in Sri lanka are of contact type encoders, While these sensors are strong departments of cost and conversion time. They lack in all other departments. It imposes considerable mechanical resistance due to contact points

      It requires complex circuitry
      resolution is 3.75 degrees, which is rather low.

b. Absolute digital encoder

While these types of encoders were the best option in terms of considered parameters, the cost was prohibitively high.

c. Incremental encoders

Incremental encoders (optical) were strong in features of resolution, Speed of conversion, and it did required complex circuitry as contact bounce was not a problem with these type of encoders. However it was again terribly expensive to be competitive in the design of a prototype laboratory model. However this is as good a option as the absolute digital encoder for the final product.

d. Simple potentiometers (Appendix G)

Simple potentiometers were strong in departments of cost and resolution (determined by the A to D word length only) and it needed a simple low pass filter to attenuate high frequency components generated by contact bounce. But linearity was a concern for simple potentiometers. Conversion speed was extremely good and was determined by the speed of the A to D converter.
But simple potentiometers also impose a mechanical resistance due to contact friction.

e. Absolute analog encoders contact less type (Appendix H)

These are a type of RVDTs, it produces an analog output (0-5V) depending on the shaft angle (0-360)
This type of encoders eliminate excessive noise due to contact bounce, does not impose mechanical friction due to slider contacts. But they are relatively expensive.

f. Absolute analog encoders contact type: (Appendix I)

Absolute analog encoders offer a compromise between cost and mechanical friction. Use of double ball bearing reduces the mechanical friction imposed on the system and it is not as expensive as the contact less type

Therefore, taking into consideration all above aspects, multi turn wire wound precision potentiometer (Fig 39b) was selected for the pan movement and a single turn wire wound servo potentiometer (Fig 3.11) was selected for the tilt movement.

3.1.9 Calculating the moment of inertia seen by the pan motor
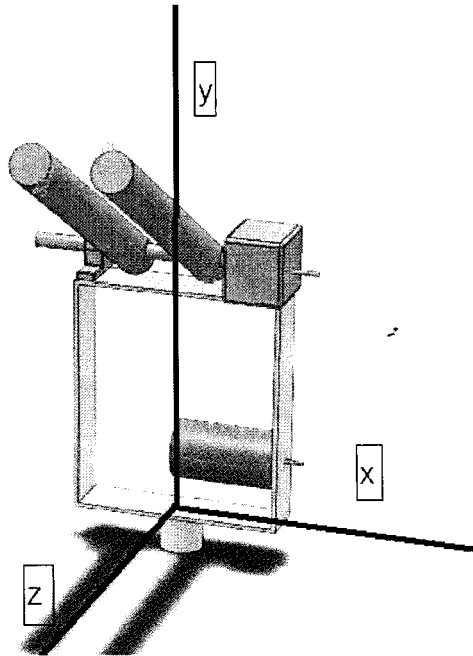
Fig3.8 calculating moment of inertia around axis y

Density of steel =7.85 g cm^3
Using 'solidworks', the moment of inertia around y axis is calculated at the center of mass is 0.07kgm^2

Parallel axis theorem

Once the moment of inertia has been calculated for rotations about the center of mass of a rigid body, one can conveniently recalculate the moment of inertia for all parallel rotation axes as well, without having to resort to the formal definition. If the axis of rotation is displaced by a distance r from the center of mass axis of rotation (e.g., spinning a disc about a point on its periphery, rather than through its center,) the displaced and center-moment of inertia are related as follows:

$$I_{displaced} = I_{center} + mr^2 \qquad (3.1)$$

According to the solid works model the center of rotation is displaced from the centre of mass by a distance of 0.02 m and the weight of the system is 7.86 kg. Therefore;

$$r = 0.02$$
$$m = 7.86$$
$$I_{Center} = 0.07 kgm^2$$

18

$$I_{displaced} = 0.07 + 0.003144$$

$$I_{displaced} = 0.073144 \ kgm^2$$

(3.2)

This value should be divided by a factor of $(70.8)^2$ which is the square of the gears ratio

Reflected interia on the motor shaft $= (0.073144 \ kg.m^{2)}/ (70.8)^2$

  $= 1.39 \times 10^{-5} \ \textbf{kg/m}^2$

Which is comparable with the rotor inertia of; $3.26 \times 10^{-6} \ kg/m^2$

Therefore the total inertia seen by the motor is its own inertia + load inertia

  $= 0.00001716 \ kg/m^2$

3.2 Vision System

The machine vision software used is called roborealm. Roborealm is a powerful robotic vision software application for use in computer vision, image processing, and robot vision tasks. Using an easy to use point and click interface complex image analysis and robot control is achieved.

Roborealm interface screen consists of three main windows;

   1. processing pipe line window
   2. Current image window
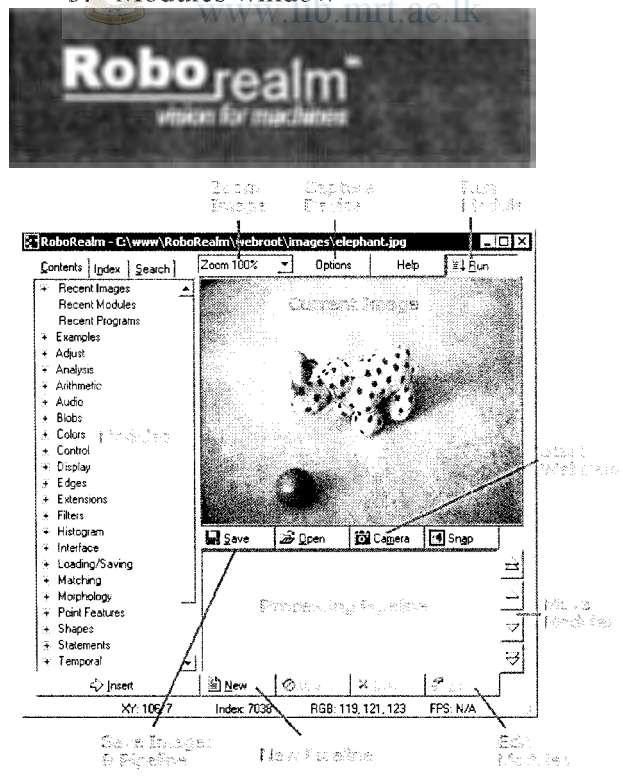   3. Modules window

Fig 3.9 Roborealm Startup screen

Modules can be dragged and dropped from "modules" window to "processing pipeline". When the program starts "roborealm" will carry out all the modules in the processing pipeline in sequence.

3.2.1 Pipe Program

Flow diagram for the pipe program is given below.

Step1.
```
┌────────────────────────────────────┐
│   Filter moving pixels from the    │
│   background (non moving pixels)    │
└────────────────────────────────────┘
```

Step2.
```
┌────────────────────────────────────┐
│  Calculate the center of gravity of the │
│            moving pixels            │
└────────────────────────────────────┘
```

Step3.
```
┌────────────────────────────────────┐
│  Carry out VB script commands       │
│  1.  Recalculate Centre Of Gravity  │
│      wrt the center of screen       │
│  2.  scale COG obtained in pixel    │
│      distances to real distances(for│
│      this camera projection         │
│      characteristics should be      │
│      known)                         │
│  3.  Convert Cartesian COG          │
│      coordinates to polar COG       │
│      coordinates (Pan angle ant Tilt│
│      angle)                         │
│  4.  Format the parameters into     │
│      suitable format for transmission│
│      over RS232                     │
└────────────────────────────────────┘
```

Step4.
```
┌────────────────────────────────────┐
│  Transmit over Rs 232 to pan tilt servo │
│            controller               │
└────────────────────────────────────┘
```
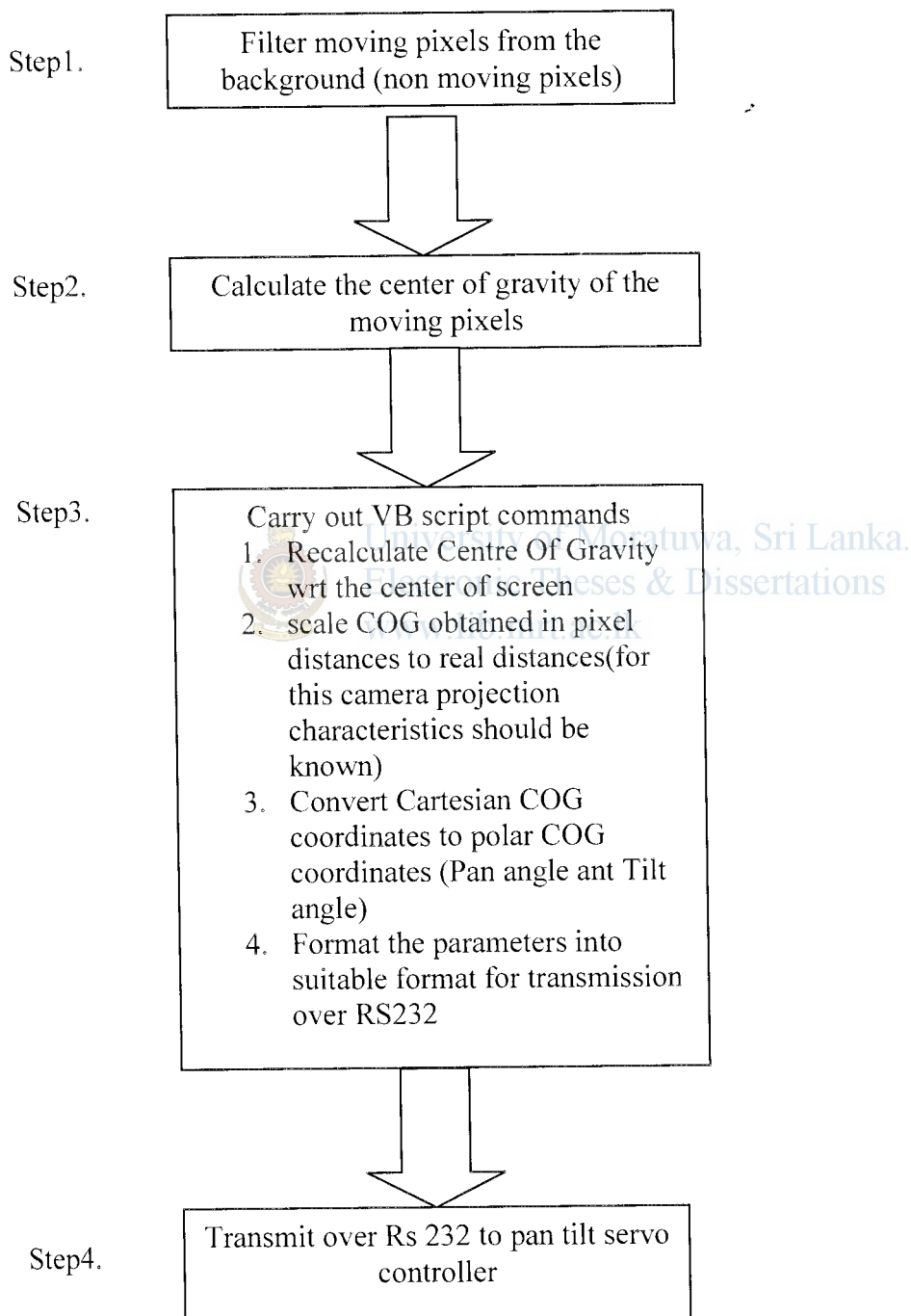
Fig 3.10 Flow diagram of the pipe program

VB scrip program (step 3) used to achieve components in step 3 is given in Appendix E.

Controller Design

4.1 Bandwidth Calculation

The nature of the target sets the primary bandwidth requirement. When the target moves, the tracking system needs to follow its every movement faithfully in order to keep the target centered on the gun turret firing axis. This requirement imposes certain demands on the system. Therefore we need to calculate the maximum frequency of the target movement profile as well as calculate at what rate the mechanical system can rotate in order to track the target.

Therefore we will be looking a,t the
required bandwidth and the available bandwidth

Available bandwidth need to be higher than the required band width for satisfactory performance. In order to calculate (1), a specific target aircraft is selected. (A10 Thunder bolt ground attack craft) then its movement characteristics are analysed to obtain the maximum demand it will impose on a tracking system. A reasonable tracking distance is selected as the minimum tracking distance.

For calculating the available bandwidth, sinusoidal inputs of increasing frequency is imposed on the system and its response amplitude measured. By analyzing the input vs output amplitude, available band width is calculated.

4.1.1 Required Bandwidth of the system

Low level anti aircraft artillery will come in to effect only when the target is within its strike range, a typical short range AAA is effective within a distance of approximately 3000 m. Specifications of a typical AAA (PGZ95) is given below for reference

Specifications of PGZ95

Crew:	5
Calibre:	25mm
Muzzle Velocity:	1,050m/s
Effective Range:	3,200m
Rate of Fire:	600~700 rounds/min

Next we must determine the type of target this AAA turret is going to engage: typically low flying ground attack aircraft are military aircraft designed to attack targets on the ground and are often deployed as close air support for, and in proximity to, their own ground forces. The proximity to friendly forces requires precision strikes from these aircraft that are not possible with typical bomber aircraft. Ground –attack aircraft are helicopters or fixed wing turbo props.

However at such low levels these aircraft (particularly jet fighters) cannot achieve their top speeds. Therefore we will take the specifications of a typical ground attack craft, the A-10 Thunderbolt.

A-10 thunder bolt has a maximum speed of 187 m/s, and assuming a maximum G force of 4 g's (which is extremely unlikely at low levels) following velocity profile (fig 2.5) is constructed for the said aircraft.
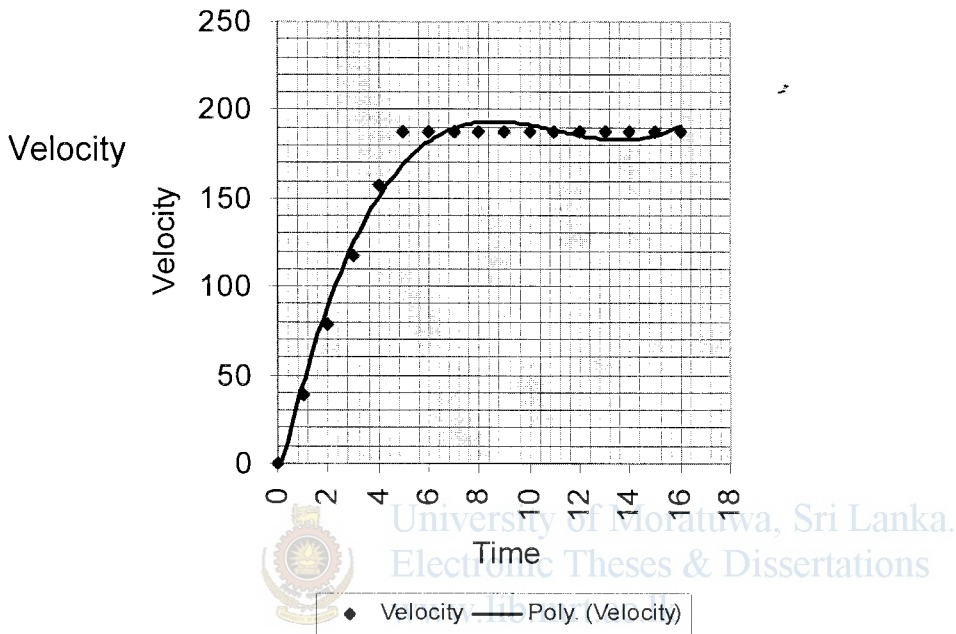
A-10 Thunderbolt movement profile

Fig 4.1 velocity profile of an A10 thunder bolt at maximum acceleration

The third order velocity profile polynomial of the above movement takes the form;

$$V = at^3 + bt^2 + ct + d \qquad (4.1)$$

Therefore coefficients calculated using regression techniques are;

$a=$ 0.16
$b=$ -5.63
$c=$ 59.49
$d=$ -8.36

By integrating the velocity profile once over time, we end up with the position movement profile.
Ie:

$$Y = a\frac{t^4}{4} + b\frac{t^3}{3} + c\frac{t^2}{2} + dt + cons \tan t \qquad (4.2)$$

$$Y = 0.04t^4 - 1.88t^3 + 29.75t^2 - 8.36t + cons \tan t \qquad (4.3)$$
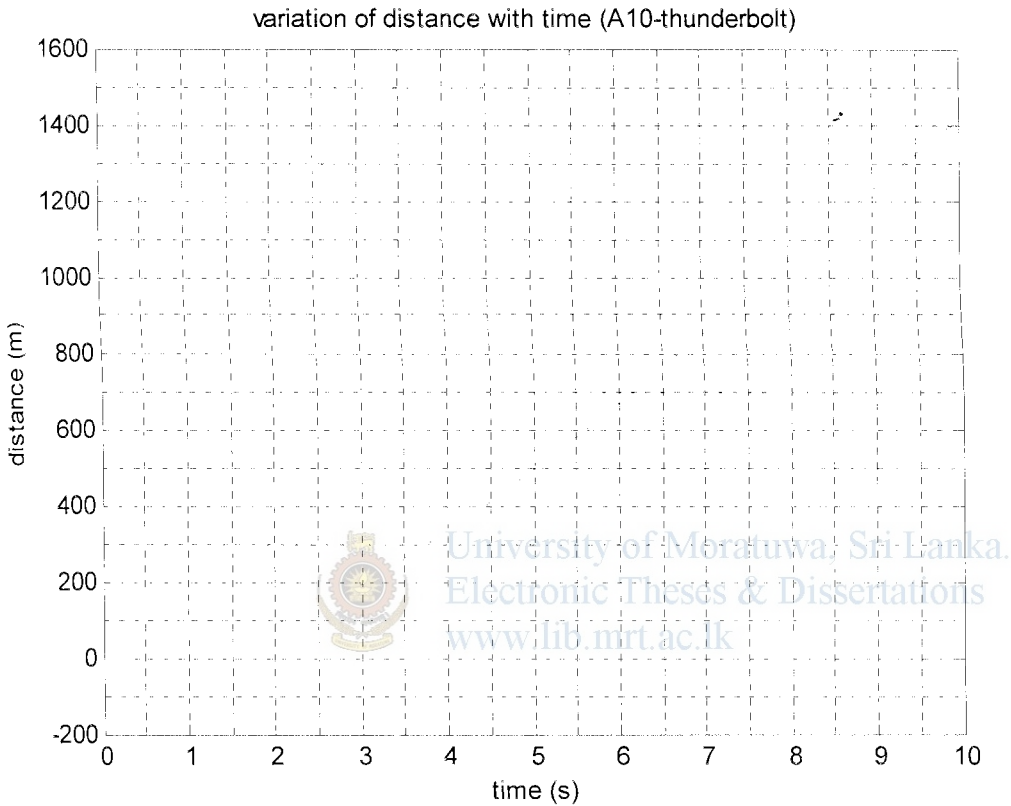

Fig 4.2 movement profile of the A-10 thunder bolt at maximum acceleration

Above equation is in the form;

$$Y = At^4 + Bt^3 + Ct^2 + Dt + E$$

But we know E = 0 (initial velocity)

Hence;

$$
\begin{aligned}
A &= \quad 0.04 \\
B &= \quad -1.88 \\
C &= \quad 29.75 \\
D &= \quad -8.36 \\
E &= \quad 0
\end{aligned}
$$

Above movement profile (Fig 2.6) is observed from a distance of 3000 meters from the target which is well within the targeting capabilities of PGZ95
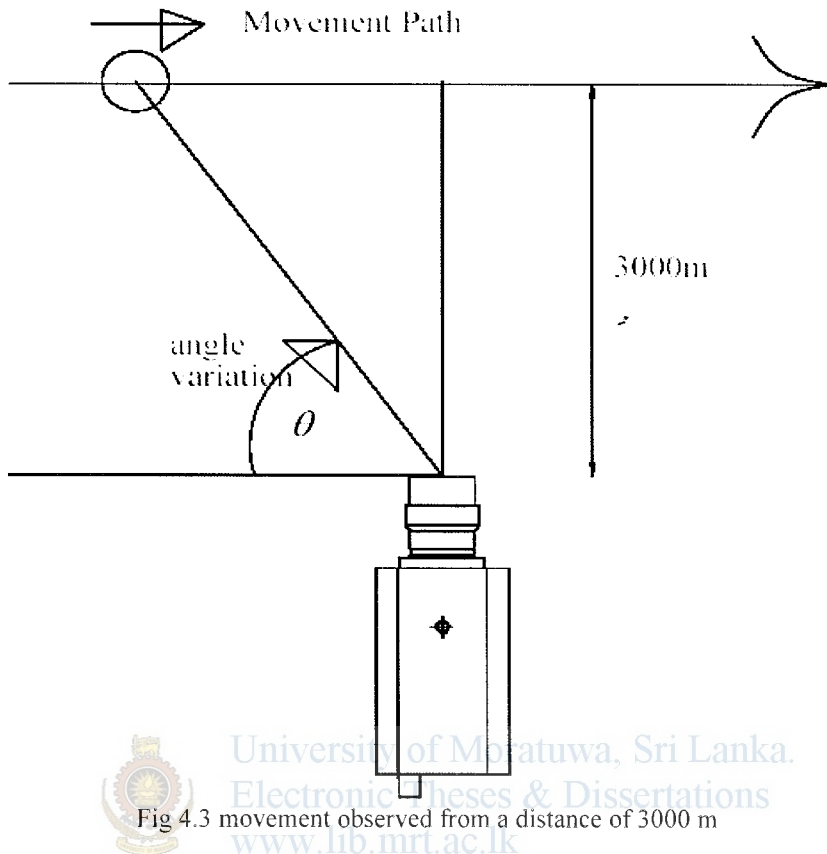

Fig 4.3 movement observed from a distance of 3000 m

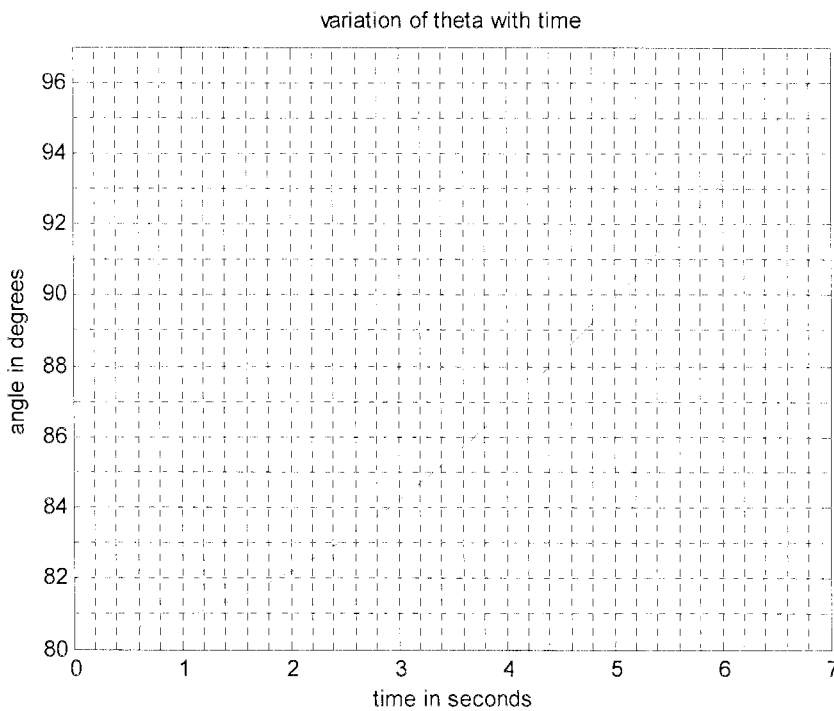Pan angle of the observing base will vary as follow

Fig 4.4 Variation of pan angle when the movement is observed from a distance of 3000m

FFT analysis (see Appendix C for .m file for fft analysis) is done on the above movement (fig. 4.4) profile to obtain the maximum frequency components of the profile; using an .m file (see appendix C) following power spectrum plot is obtained for the above movement.
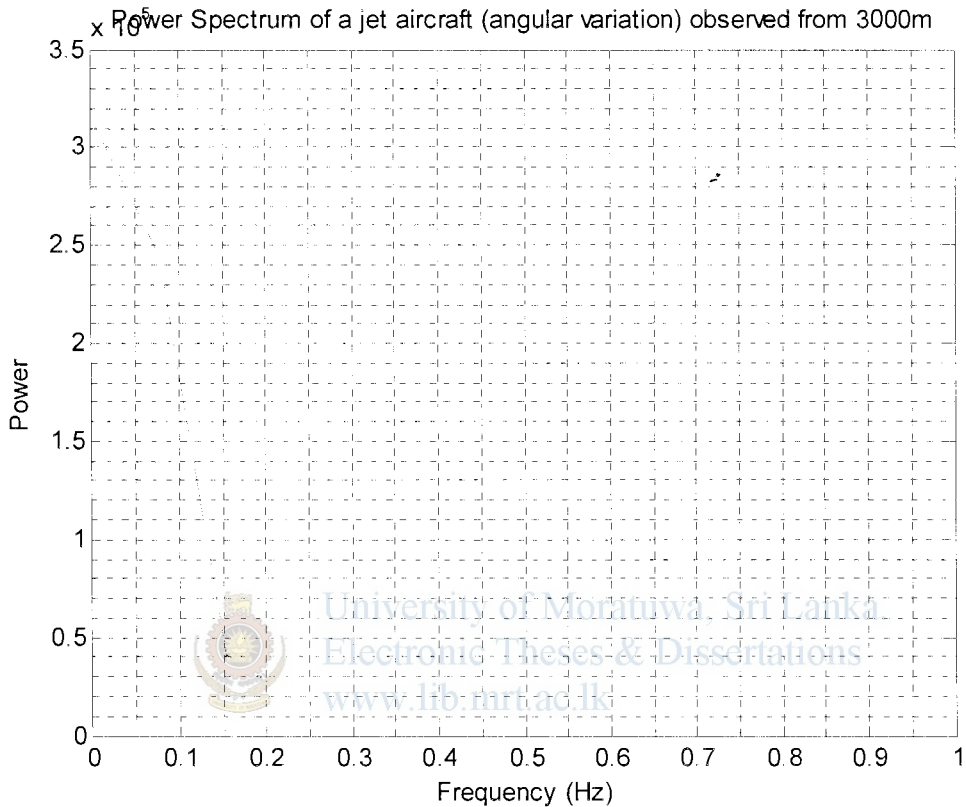

Fig 4.5 Power spectrum of the target movement

From fig.4.5 it is clear that frequency components above 1 Hz are insignificant. Therefore, pan tilt mechanism should poses a minimum band width of 1Hz (2π rad/s) or more.

This bandwidth is multiplied by the gears ratio to obtain the motor armature bandwidth.
Thereby giving a velocity bandwidth of 141.6π rad/s

Same procedure is carried out to obtain the tilt mechanism velocity bandwidth as 155π(rad/s);

Calculating the maximum angular acceleration of the movement, Maximum angular acceleration is important to calculate the maximum torque exerted on the motor armature, which will give a further guideline for motor selection.

By differentiating the angular velocity movement profile once over time, acceleration profile is obtained;

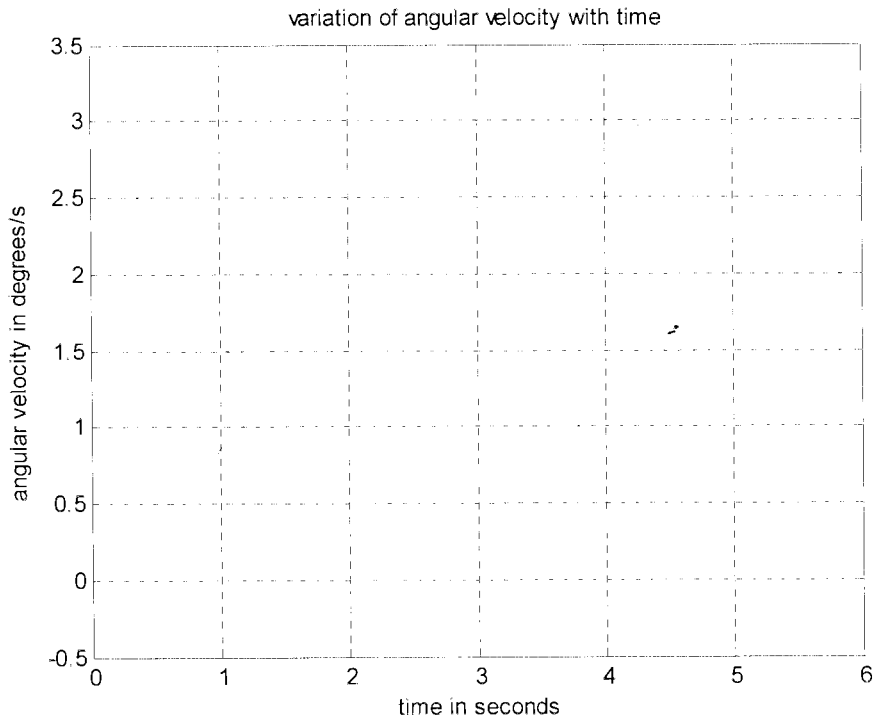variation of angular velocity with time

Fig 4.6 gives the angular velocity profile of the a10, when observed from a distance of 3000 m

By differentiating above movement profile once over time, it is possible to ascertain the angular acceleration profile of the said movement;
Ie:

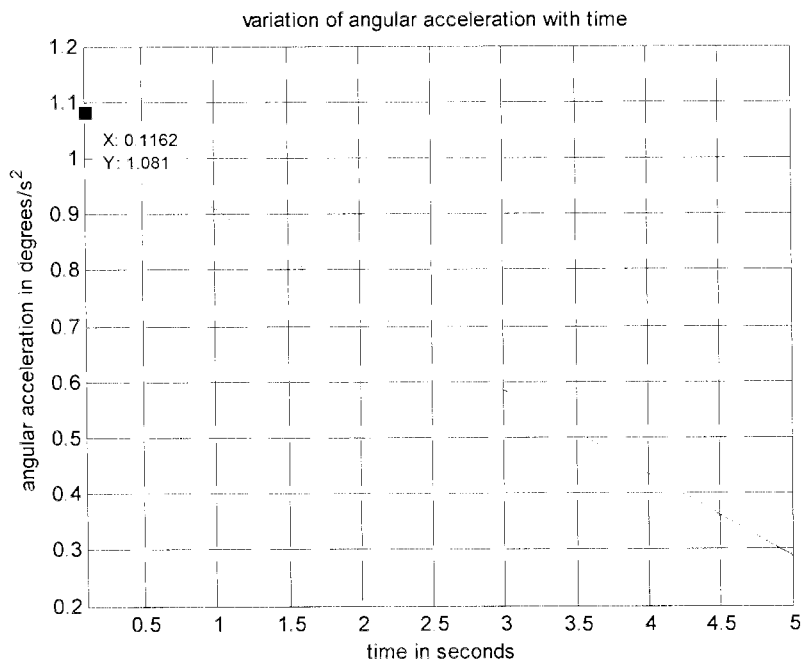variation of angular acceleration with time

Fig 4.7 angular acceleration profile

From Fig 4.7 it is clear that the maximum acceleration occurs at the beginning of the movement profile and it is 1.081 degrees / s² (0.0189 rad/s²)
Using the system inertia value of 0.00001716 kg/m², maximum torque required to achieve this acceleration is calculated as follows;

$$\tau = J\alpha \qquad (4.4)$$

Where τ is the torque require, J system inertia and α is maximum angular acceleration;
By substituting values to above equation;
Torque τ is calculated as 0.000000324324 N-m which is well within the torque capabilities of the pan movement motor (which has a maximum torque of 0.33 N-m).

4.1.2 Available Bandwidth of the Mechanical System

To ascertain its band width, sinusoidal inputs of increasing frequency was applied and the corresponding response measured
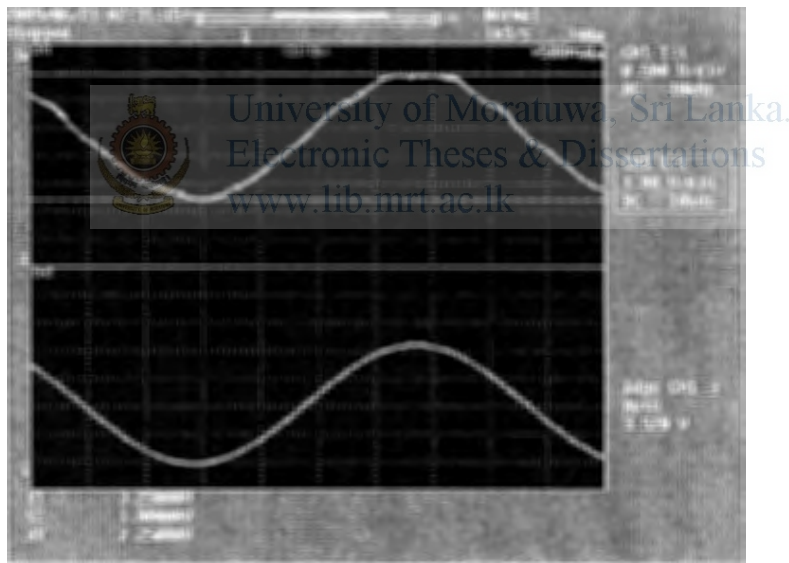

Fig 4.8 (a)

Fig 4.8 (a) shows the system response to sinusoidal input of 0.2Hz,
Channel 3 (bottom trace) shows the input signal, Channel 1 (top trace) shows the output response.

Fig4.8 (b)

Fig 4.8 (b) shows the system response to sinusoidal input of 0.28Hz,
Channel 1 (bottom trace) shows the input signal, Channel 2 (top trace) shows
the output response.

Fig 4.8 (c)

Fig 4.8 (c) shows the system response to sinusoidal input of 0.4Hz,
Channel 1 (bottom trace) shows the input signal, Channel 2 (top trace) shows
the output response.

Fig 4.8 (d)

Fig 4.8 (d) shows the system response to sinusoidal input of 0.48Hz,
Channel 1 (bottom trace) shows the input signal, Channel 2 (top trace) shows
the output response.
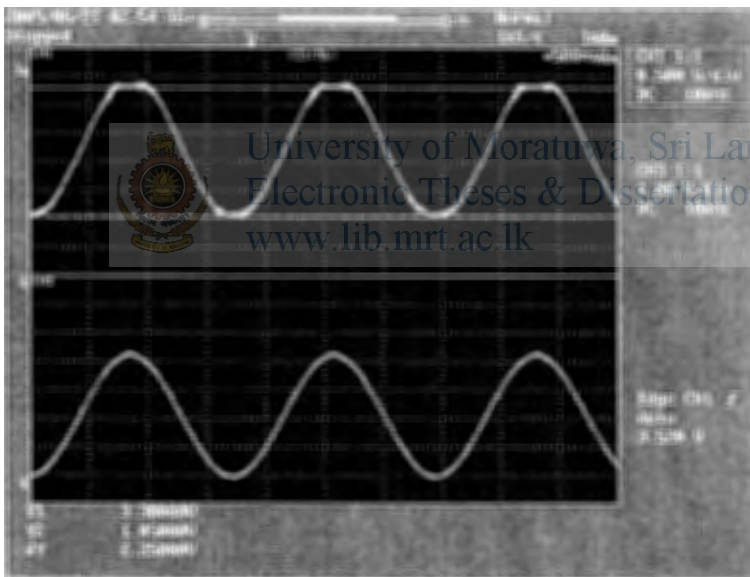
Fig 4.8(e)

Fig 4.8(e) shows the system response to sinusoidal input of 0.58Hz,
Channel 1 (bottom trace) shows the input signal, Channel 2 (top trace) shows
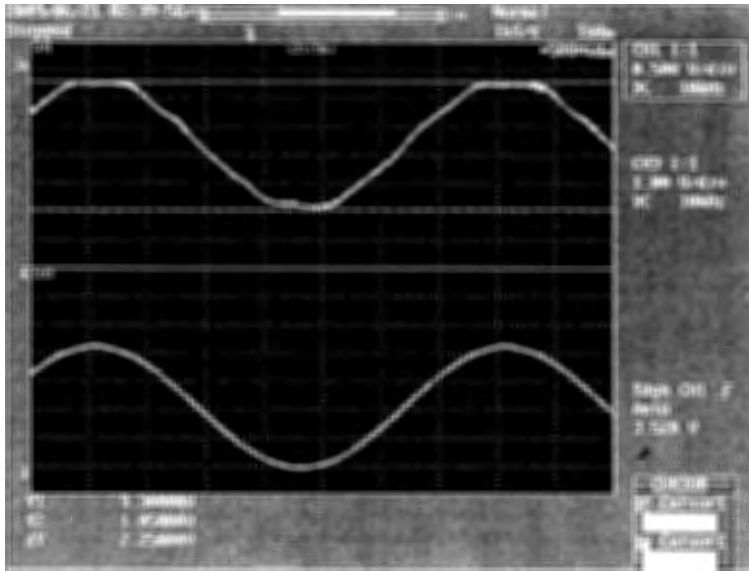the output response.
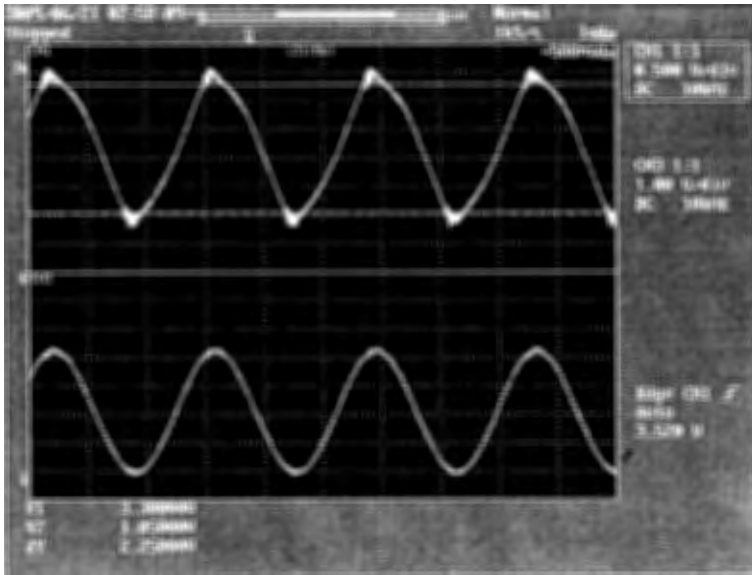
Fig 4.8 (f)

Fig 4.8 (f) shows the system response to sinusoidal input of 0.73Hz, Channel 1 (bottom trace) shows the input signal, Channel 2 (top trace) shows the output response.
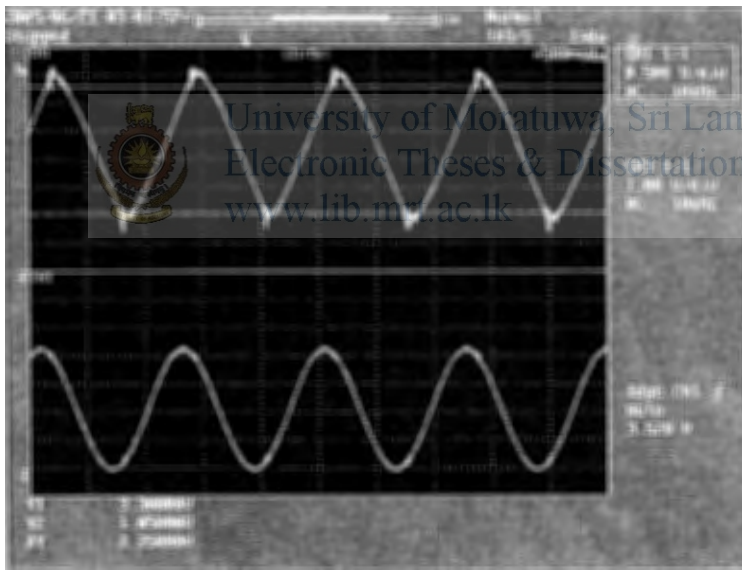
Fig 4.8 (g)

Fig 4.8 (g) shows the system response to sinusoidal input of 0.81Hz, Channel 1 (bottom trace) shows the input signal, Channel 2 (top trace) shows the output response.
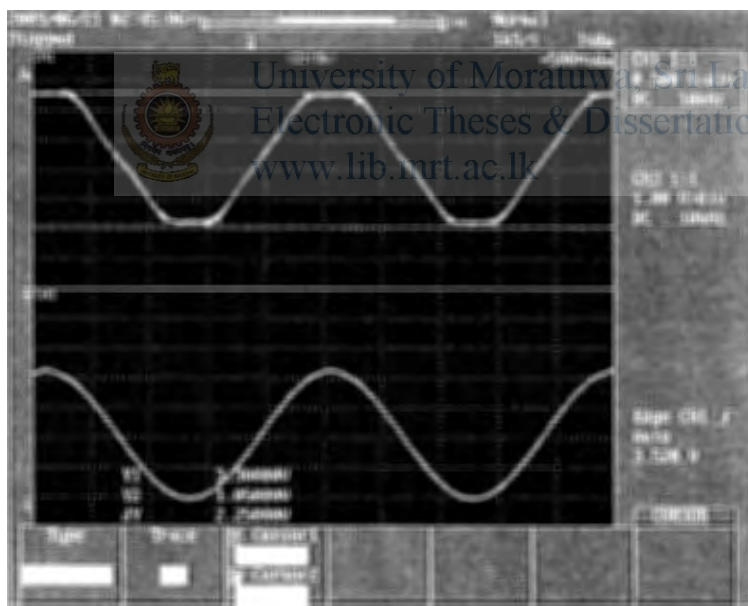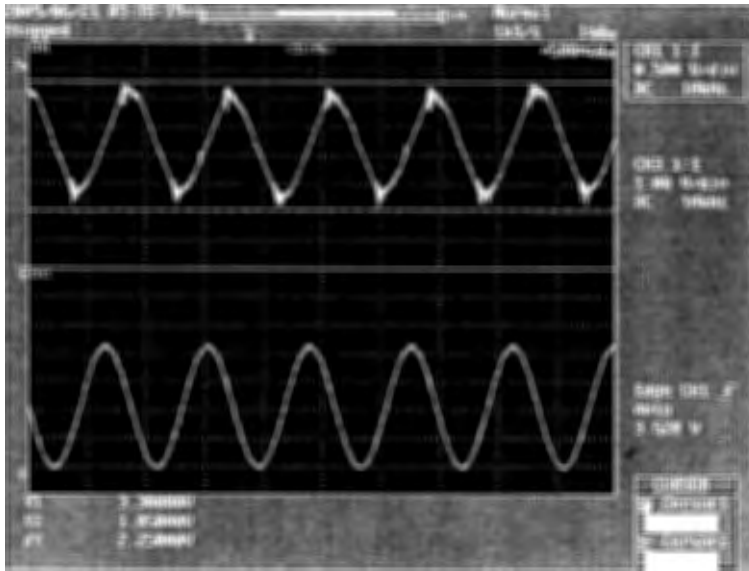
Fig 4.8 (h)

Fig 4.8 (h) shows the system response to sinusoidal input of 1.15Hz,
Channel 1 (bottom trace) shows the input signal, Channel 2 (top trace) shows
the output response.
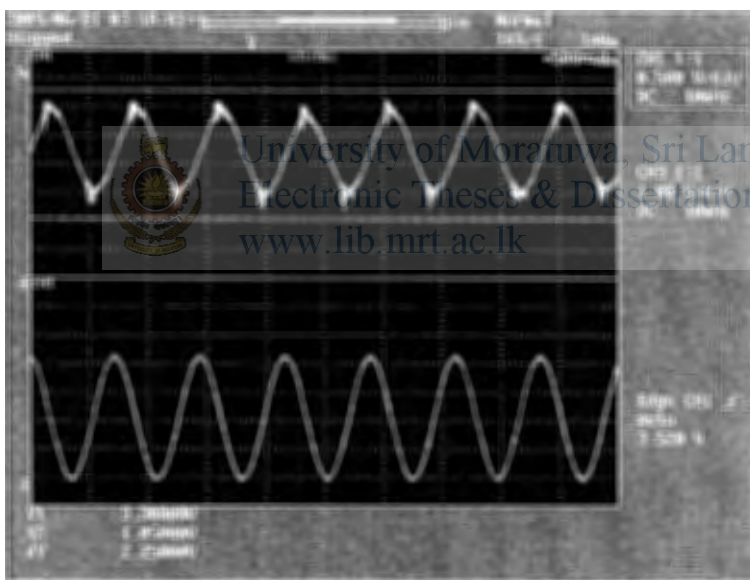
Fig 4.8 (i)

Fig 4.8 (i) shows the system response to sinusoidal input of 1.36 Hz,
Channel 1 (bottom trace) shows the input signal, Channel 2 (top trace) shows
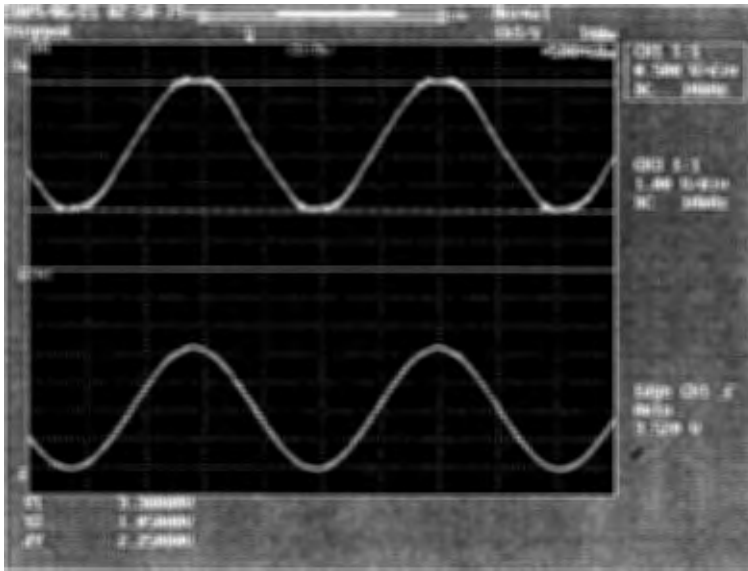the output response.

31

Mechanical bandwidth of the system is obtained by plotting the gain against frequency.
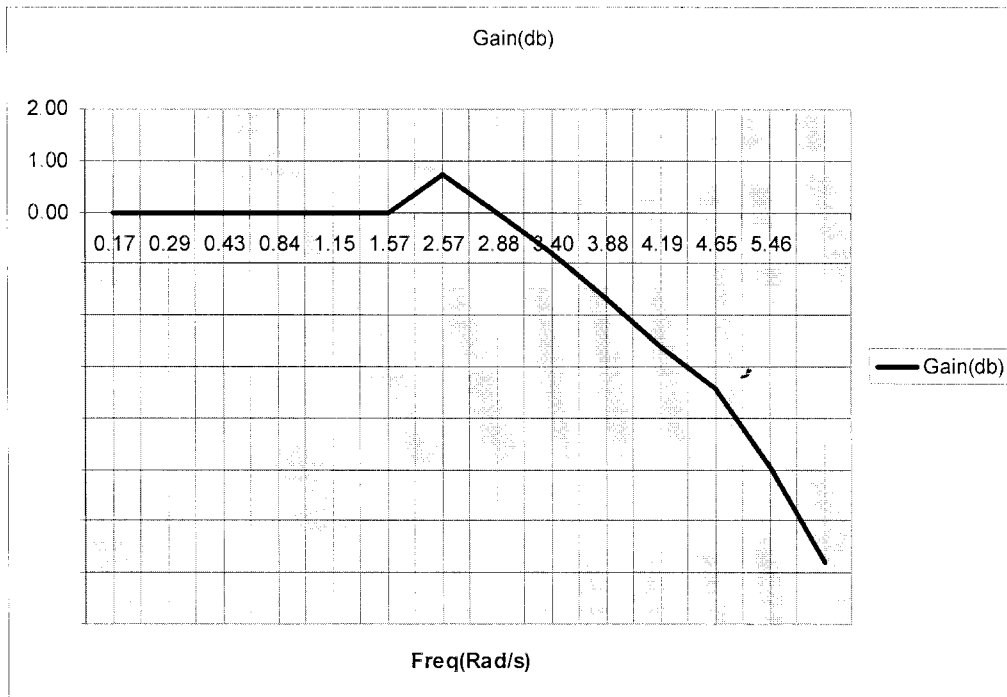
Fig4.9   Gain vs freq plot for the Pan movement.

-3dB gain occurs at 4.6 rad/s (ie: 0.73 Hz)

Ie: Available band width and required band with is comparable for satisfactory operation.

4.2 Design of Electronic Hardware

4.2.1 Overview of the Control Architecture

The controller is a PID type, where the set point is the pan angle input and the output is the actual angle of the mechanism
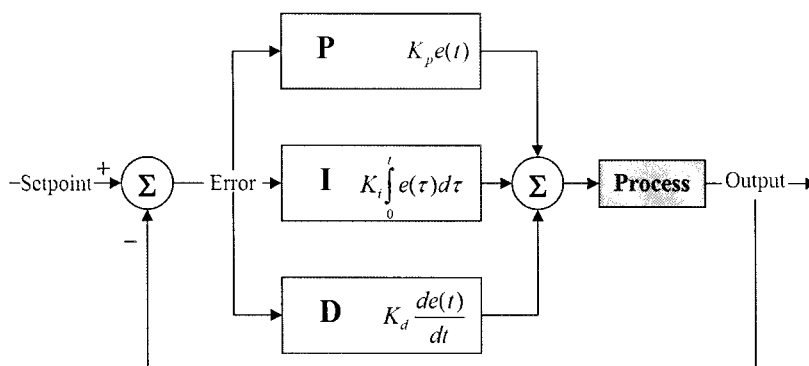
Fig 4.10 PID Controller and plant

Block diagram of the control architecture;
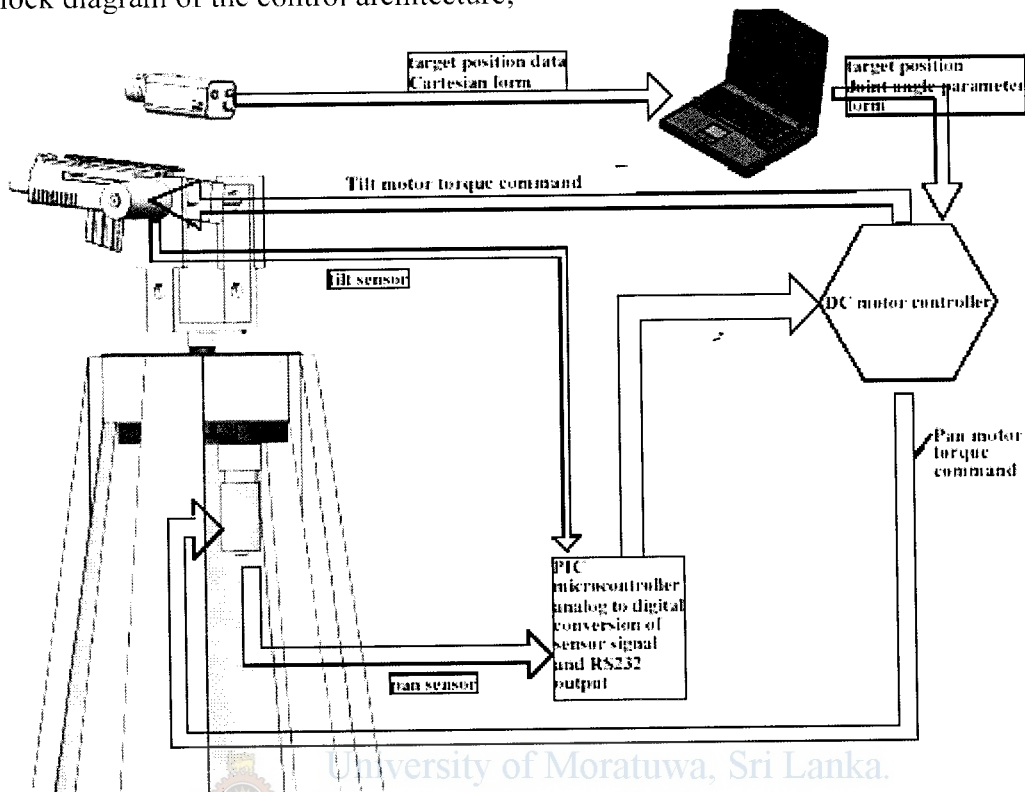
Fig 4.11 Overall control architecture of the system

Fig 4.11 shows the overall control architecture of the system. Components in the design architecture;

- Micro controller based Sensor ADC circuit
- Micro controller based PID compensator
- H-Bridge for driving the DC motor
- Microcontroller based Interface PCB for communication with target tracking system

4.2.2 Micro Controller Based Sensor ADC and PID Compensator.

Analog to digital converter and PID compensator was implemented on a single micro controller (PIC16f877A) the PCB was designed with a
- 5 V voltage regulator for supply
- 8 pin connector header for data port input
- 5 pin connecter header for ICSP (in circuit serial programming)
- L298D motor control driver (initial design)
- 2 pin header connector for sensor input
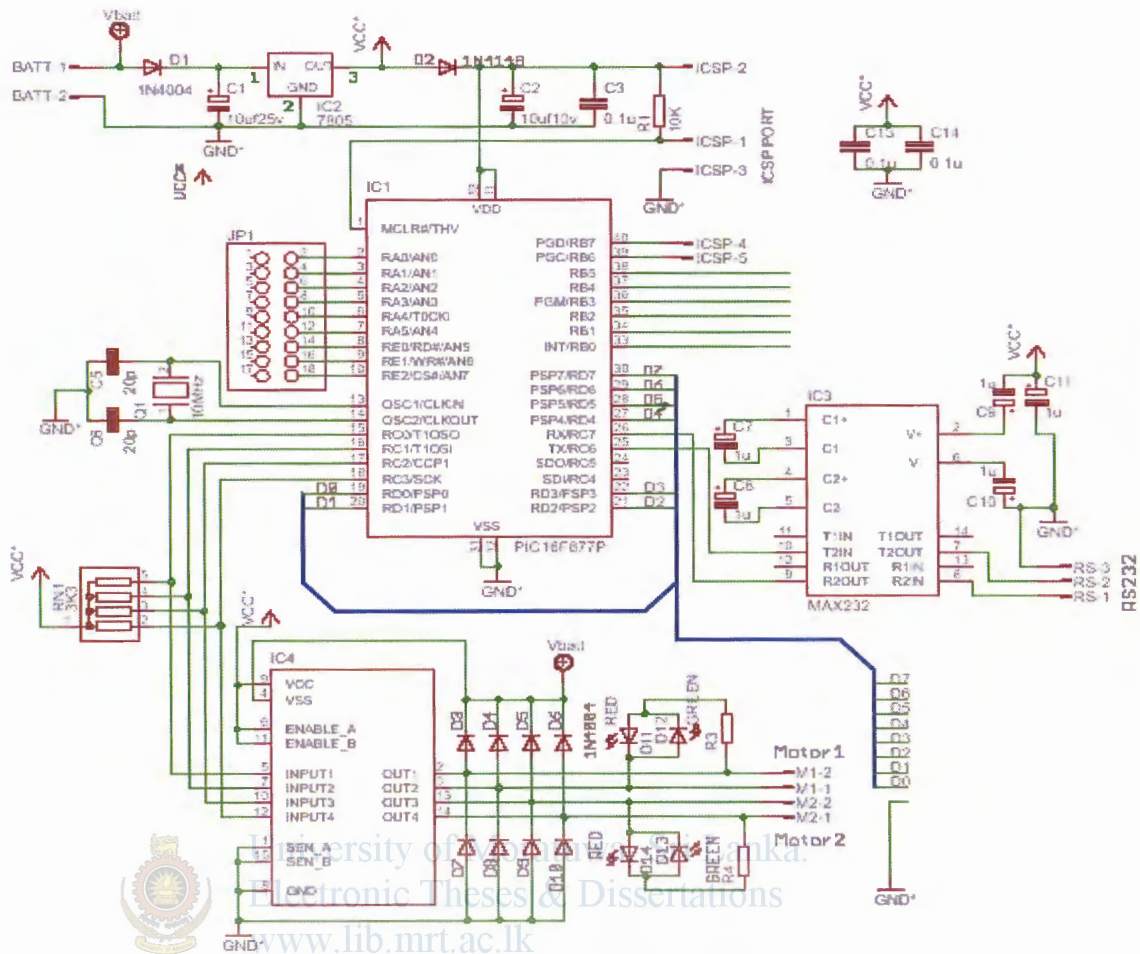
Fig4.12   schematic diagram of PIC16F877A micro controller support PCB used for sensor inputs and PID compensator
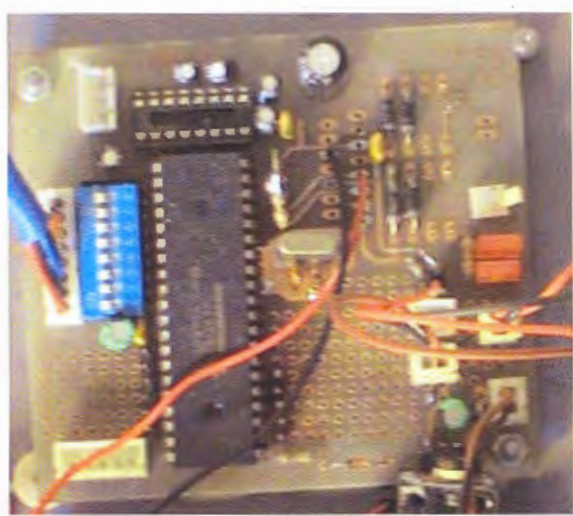
Fig 4.13   Microcontroller PCB populated with components

4.2.3 H-Bridge

H-Bridge has following characteristics.
- Peak Current Handling capacity 8 A
- Regenerative braking mode
- Two control inputs

Inputs		Result on the connected motor
W1	W2	
0	0	Motor is free wheeling (High impedance)
0	1	Turning clockwise
1	0	Turning Anti clockwise
1	1	Active breaking (regenerative mode)

Table 4.1 Truth table for H bridge

The H-Bridge is actuated by a PWM signal. The motor can be operated in two ways with PWM signal.

Mode 1:   The motor can be stopped during PWM off state (regenerative breaking mode)

Mode 2:   The motor can be allowed to free wheel during off state.

Each mode has advantages and disadvantages. Mode 2 has the advantage of less electrical stress exerted on output stages hence allowing for less complex electronics design. But it has the disadvantage of excessive over shoot possibly leading to instability. Mode 1 exerts high electrical stress (current spikes) during direction changes and sudden stops. But due to active breaking overshoot is limited and demonstrates better tracking performance, hence mode 1 is used in this project
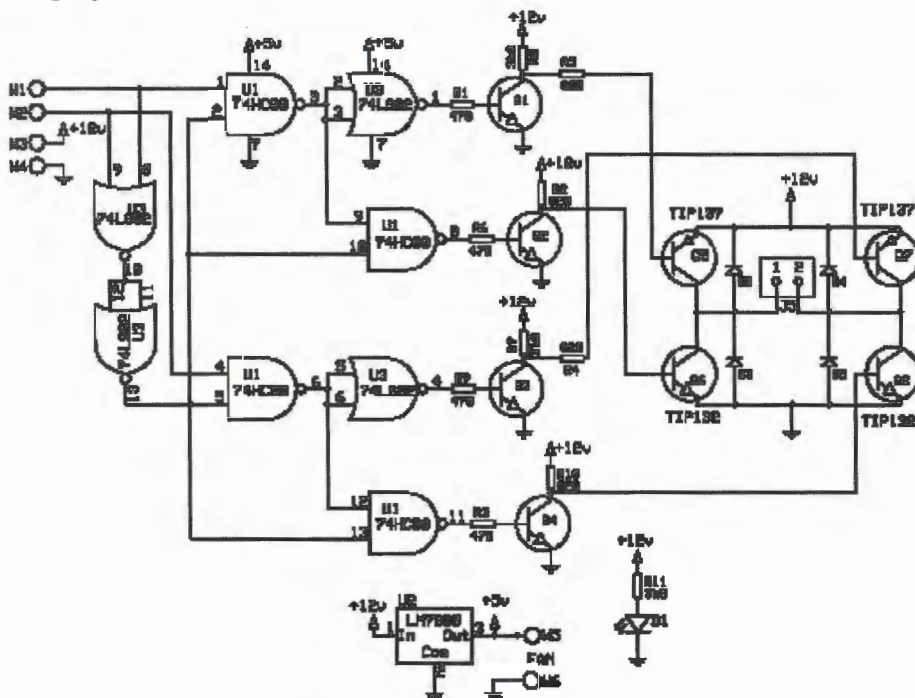
Fig 4.14(a) schematic diagram of the H-Bridge (Source: www.ikalogic.com)
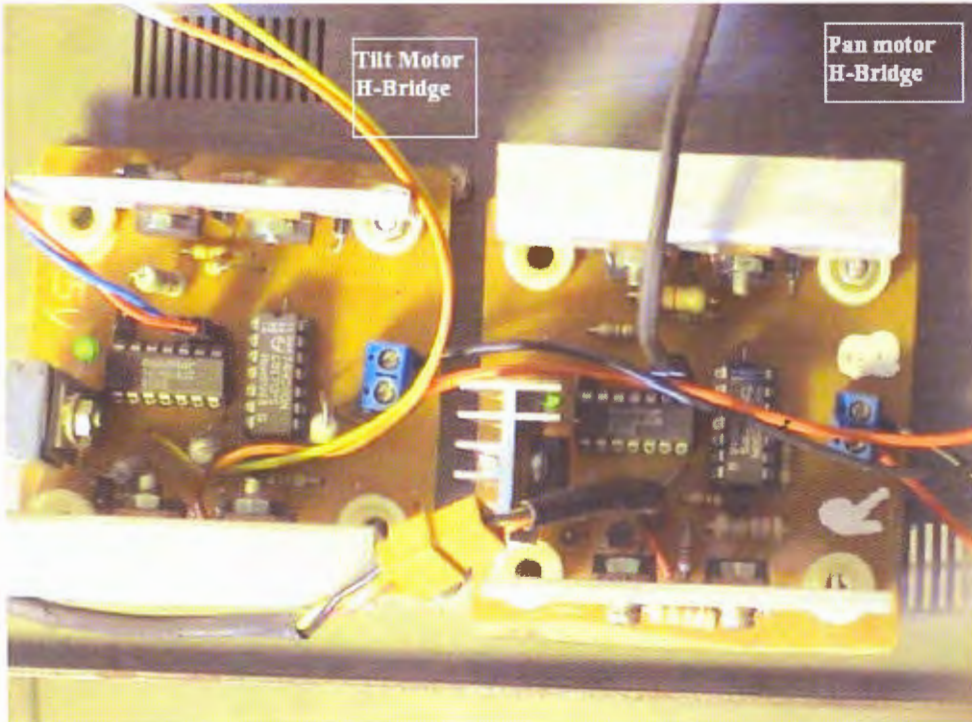
Fig 4.14 (b) H- Bridge PCB populated with components (two units for Pan Movement and tilt movement)

4.2.4 Interface Board

Interface board is used for communication with the target tracking system. In this case the computer which implements machine vision software. It is based on Atmel 89s8252 microcontroller. This has 4 I/O ports. It receives the coded command from the Target tracking system (Radar) then it decodes the composite command to determine the joint angle variables for pan and tilt motors and places the corresponding values on relevant out put ports; i.e: port 1 is used for tilt movement and Port 2 is used for pan movement.

4.2.5 Mathematical Modeling of the System

Using equations obtained in chapter 2 for the motor/load model;

$$\tau = \eta \tau_a \tag{4.1}$$

$$\overset{0}{\theta} = \frac{1}{\eta} \overset{0}{\theta}_a \tag{4.2}$$

$$\theta = \frac{1}{\eta} \theta_a \tag{4.3}$$

36

$$\tau_a = I_{eff}\overset{oo}{\theta}_a + B_{eff}\overset{o}{\theta}_a \qquad (4.4)$$

$$L_a\frac{di_a}{dt} + R_a i_a = v - K_e\overset{o}{\theta}_a \qquad (4.5)$$

$$e = K_e\theta_a \qquad (4.6)$$

$$\tau_a = K_e i_a \qquad (4.7)$$

Following open loop simulink model is constructed using above equations.
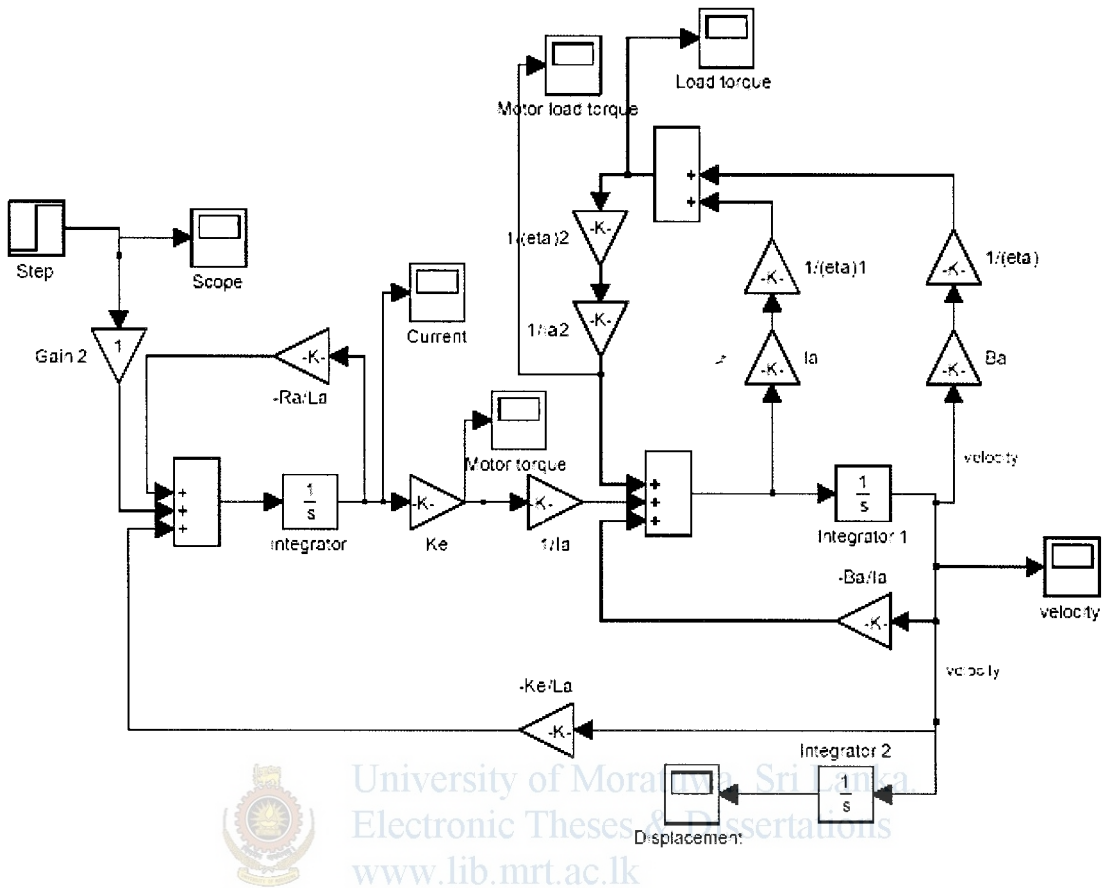
Fig 4.15 Simulink model of the complete system

This simulink model (fig 4.15) is used to obtain the transfer function of the open loop system (see section 4.1.4)

4.2.6 Estimation of Viscous Friction of the Motor Load Model.

In order to estimate the viscous friction of the system, an experimental method is used.

Output response of the actual model and the simulink model is compared and the viscous friction of the simulink model is adjusted until the output step response of both systems are identical
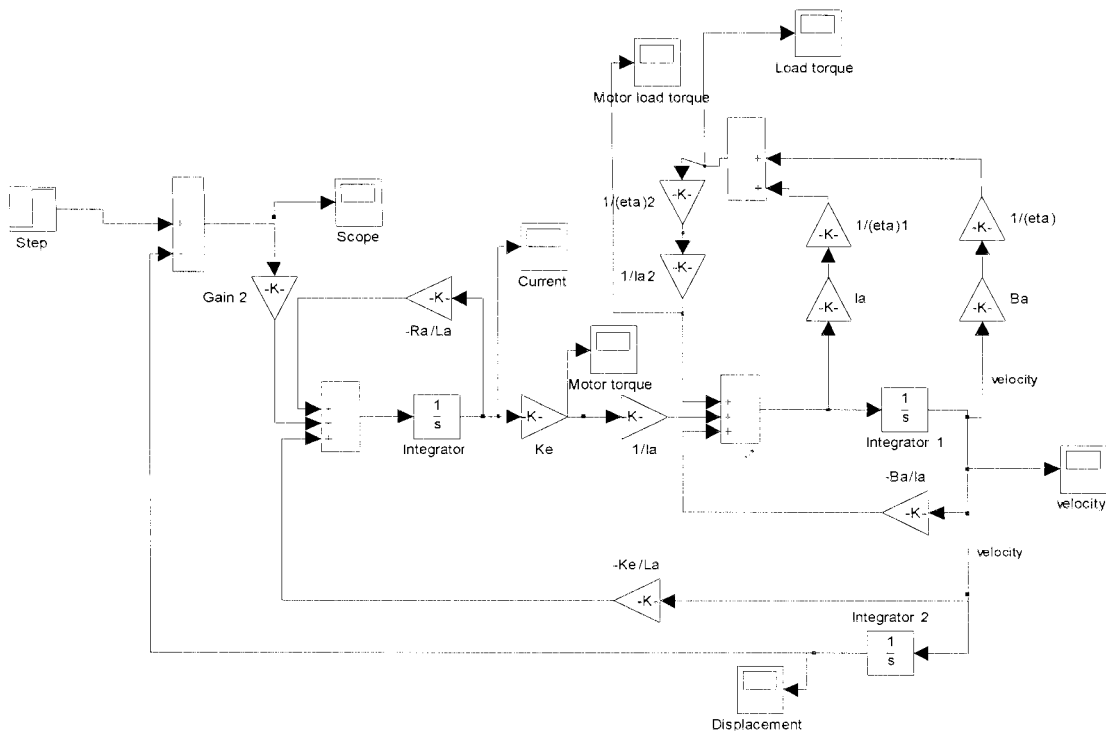
Fig 4.16 Closed loop version of the motor load model

Fig4.16 shows a closed loop version of the motor load model. In order to estimate the viscous friction and lump all non linear parameters together, Step response of the above system was compared with the actual step response of the pan movement motor. Then B_a(viscous friction coefficient) of the system was adjusted in simulink model until both step responses were identical.
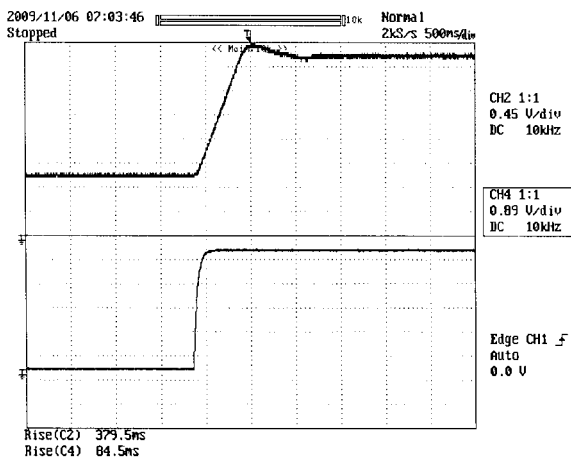
Fig 4.17 (a)   Fig 4.7 (b)

Figure 4.17 (a): Input step (bottom trace) and output response (top trace) of the actual pan Mechanism, Rise time 379ms. (b) Output step response of Simulink model, Rise time 379 ms
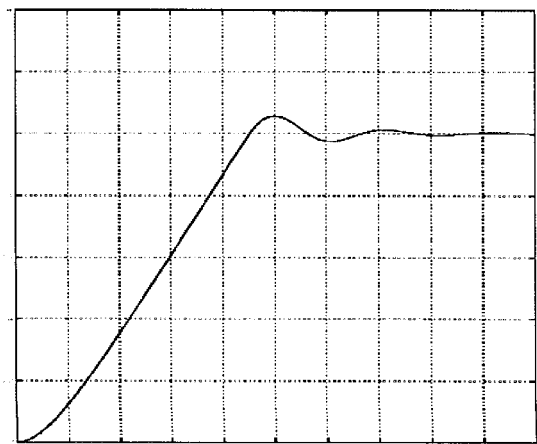
With a viscous damping factor of 0.000062 Nm s/rad, the simulink model step response is identical to the actual step response.

39

Therefore it is reasonalble to assume that the viscous damping factor of the motor load system is 0.000062 Nm s/rad.

This value is used on the above model (fig 4.5) in calculating the transfer function for the system.

4.3 Loop Shaping (Tracking Response)

Above model (Fig 4.5) is saved in the simulink environment and using "linmod" command the state space model of the above simulink model is obtained. As such, the state space model is;

$$A = \begin{pmatrix} -3.6 & 1731.1 \\ -6.3 & -1303.4 \end{pmatrix} \quad (4.8)$$

$$B = \begin{pmatrix} 0 \\ 1 \end{pmatrix} \quad (4.9)$$

$$C = (1 \quad 0) \quad (4.10)$$

$$D = (0) \quad (4.11)$$

Using matlab command;

[numcl,dencl] = ss2tf(A,B,C,D)

The velocity transfers function of the system;

$$\overset{o}{\theta} = \frac{2.274 \times 10^{-14} S + 1731}{S^2 + 1307S + 15700} \quad (4.12)$$

Step response of the velocity transfer function is given by Fig 4.18, step response saturates at 0.11 in response to a step input of unity, this is due to attenuation of the system. The design attempts to measure this attenuation from the bode plot fig 4.19.
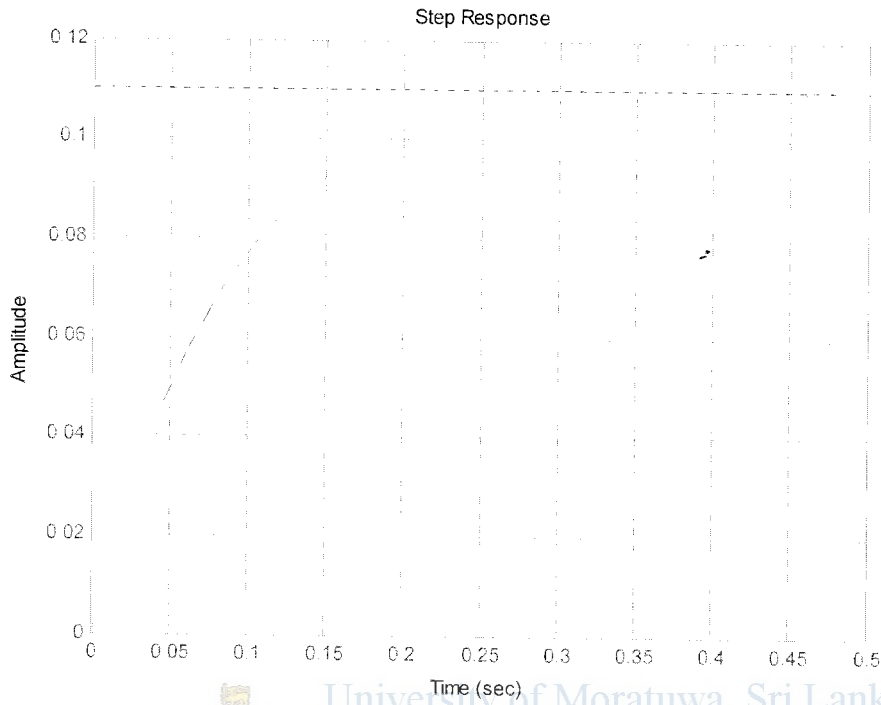
Fig4.18 the velocity step response of the system
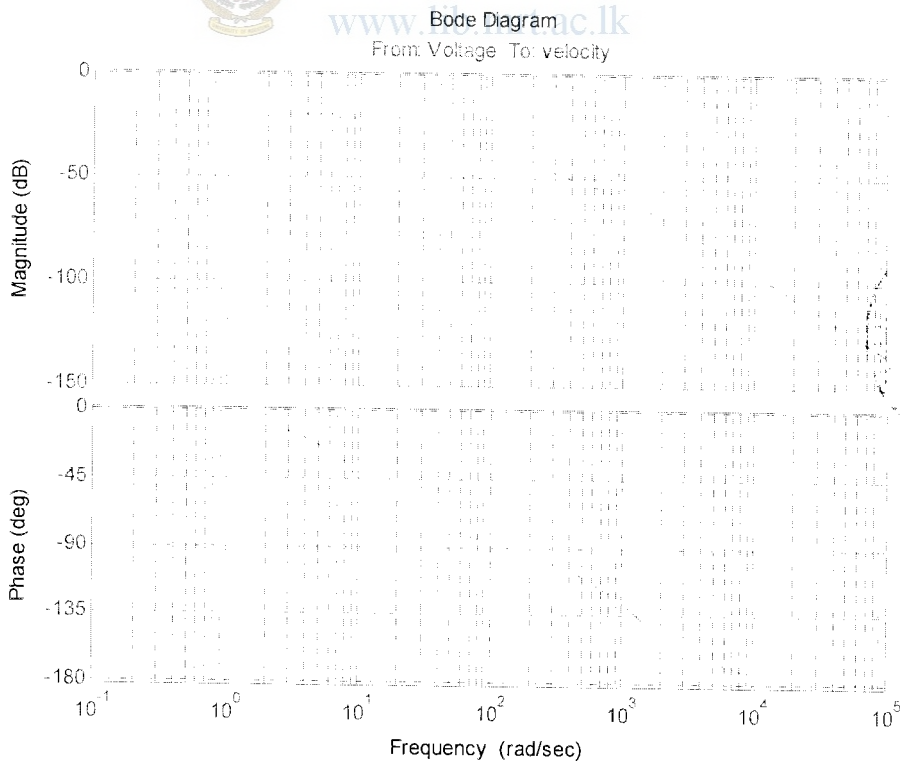
Fig4.19 shows the bode plot of the system

The angular position transfer function

$$\theta = \frac{2.274 \times 10^{-14} S + 1731}{S^3 + 1307S^2 + 15700S} \qquad (4.13)$$

the system has a 30dB (approx) attenuation at 0 Hz;
Required bandwidth is obtained by shaping the above bode diagram (Fig 4.19)
From chapter 2.3, required bandwidth is 141.6π rad/s or 444.26 rad/s (Pan movement)
A simple gain K is used in the forward path to get the required bandwidth.

From the bode plot it is seen that the gain at 444.26 rad/s is -50.9 db

To get -3db at 444.26 rad/s
$$20 \log K - 50.9 dB = -3 dB$$

therefore;
$$K = 10^{47.9/20} \qquad (4.14)$$

$$K \approx 249$$

The H-Bridge has a natural gain of approximately 5 therefore the forward gain required from the controller is ≈ 50

Drawing again the gain and phase plot with a gain of 249 in the forward path, gives;
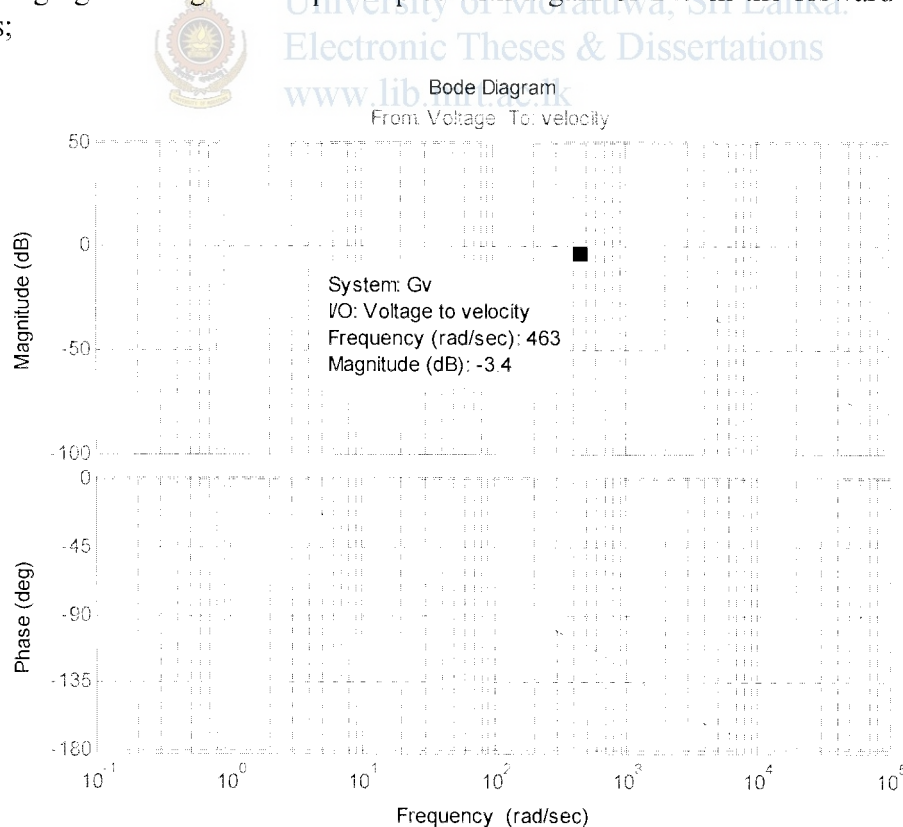
Fig 4.20 gain and phase plot with a gain of 249 in forward path

With a gain of 249 in the forward path, the approximate gain at 444.6 rad/s is -3db, thereby giving the system required band width.

4.4 Stability of the System

Fig4.21 Phase margin 82 deg

According to Fig 4.21 Phase margin is +82deg and the phase angle never reaches 180, which means that the system is inherently stable for all frequencies and all gains.

4.5 System with Position Feedback

Fig 4.22 shows the closed loop system with position feed back.

Velocity and Position response for Step input

A step input is fed to the closed loop system (with position feedback) and the output response of the velocity and position is observed. Fig 4.23(a) shows the velocity response and Fig 4.23(b) shows the position response.
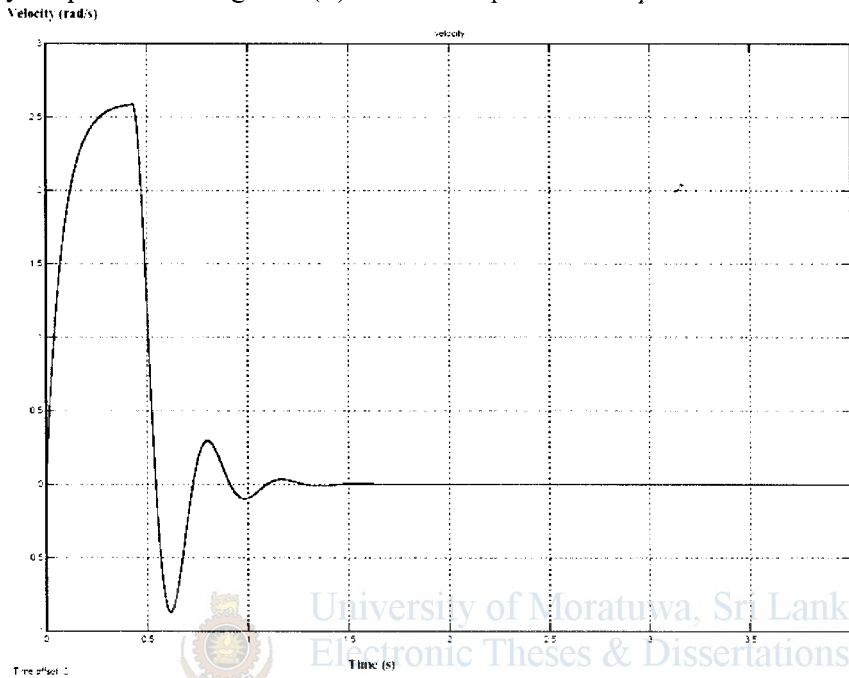
Velocity (rad/s)
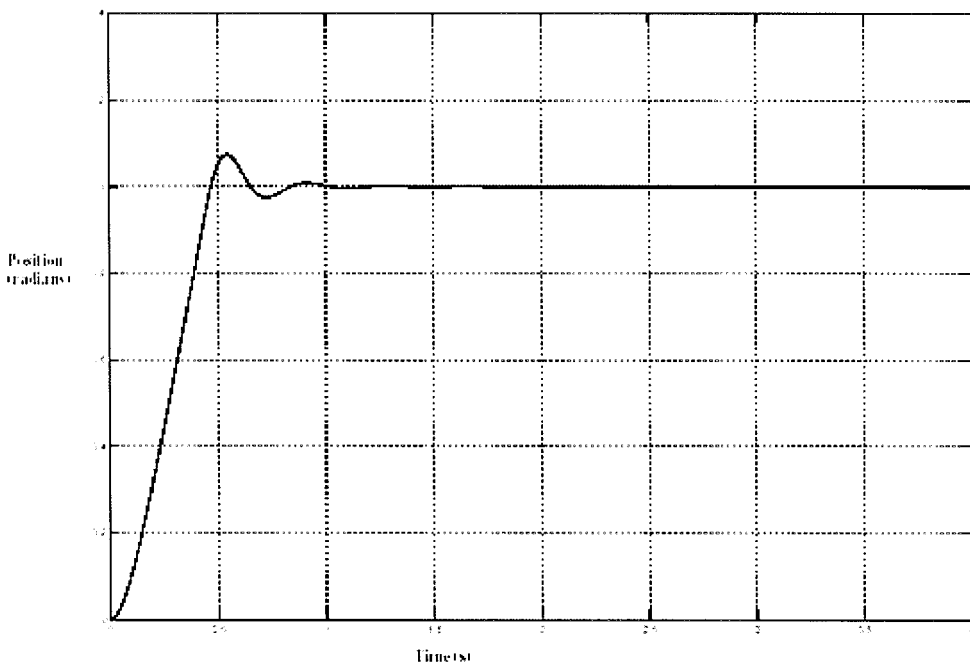
Fig 4.23(a)

Fig4.23 (b)

Fig4.23 (a)Shows the output velocity response with a calculated gain of 249. Fig4.23(b) the position step response of the compensated system

44

4.6 Digital Controller

The chosen controller is of PID form as follows;

$$D(s) = K_p + K_d s + \frac{K_i}{s} \tag{4.15}$$

Using Bilinear Transformation;

$$s = 2\frac{z-1}{T_s(z+1)} \tag{4.16}$$

Gives ;

$$D(z) = K_p + 2K_d\frac{z-1}{T_s(z+1)} + \frac{K_i}{2}\frac{T_s(z+1)}{z-1} \tag{4.17}$$

Simplifying;

$$D(z) = \frac{K_p(z-1)(z+1) + \dfrac{2K_d(z-1)(z-1)}{T_s} + \dfrac{K_iT_s(z+1)(z+1)}{2}}{(z+1)(z-1)} \tag{4.18}$$

$$D(z) = \frac{K_p(z^2-1) + \dfrac{2K_d(z^2-2z+1)}{T_s} + \dfrac{K_iT_s(z^2+2z+1)}{2}}{z^2-1} \tag{4.19}$$

$$D(z) = \frac{\left(K_p + \dfrac{2K_d}{T_s} + \dfrac{K_iT_s}{2}\right)Z^2 + \left(K_iT_s - \dfrac{4K_d}{T_s}\right)Z + \left(\dfrac{2K_d}{T_s} + \dfrac{K_iT_s}{2} - K_p\right)}{z^2-1} \tag{4.20}$$

Therefore;

$$D(z) = \frac{\left(K_p + \dfrac{2K_d}{T_s} + \dfrac{K_iT_s}{2}\right) + \left(K_iT_s - \dfrac{4K_d}{T_s}\right)Z^{-1} + \left(\dfrac{2K_d}{T_s} + \dfrac{K_iT_s}{2} - K_p\right)Z^{-2}}{1 - Z^{-2}} \tag{4.21}$$

$$D(z) = \frac{b_0 + b_1z^{-1} + b_2z^{-2}}{a_0 + a_1z^{-1} + a_2z^{-2}} \tag{4.22}$$

Where;

$$a_0 = 1$$
$$a_1 = 0$$
$$a_2 = -1$$

$$b_0 = K_p + \frac{K_i T_s}{2} + \frac{2K_d}{T_s}$$

$$b_1 = K_i T_s - \frac{4K_d}{T_s}$$

$$b_2 = \frac{2K_d}{T_s} + \frac{K_i T_s}{2} - K_p$$

$$U(z) = D(z)E(z)$$

Thus;

$$U(z)(a_0 + a_1 z^{-1} + a_2 z^{-2}) = E(z)(b_0 + b_1 z^{-1} + b_2 z^{-2}) \qquad (4.23)$$

Applying inverse Z transformation;

$$a_0 u(n) + a_1 u(n-1) + a_2(u-2) = b_0 e(n) + b_1(n-1) + b_2(n-2)$$
Where;
$$e(n) = r(n) - y(n) \qquad (4.24)$$

$$u(n) = \frac{1}{a_0}(b_0 e(n) + b_1 e(n-1) + b_2 e(n-2) - a_1 u(n-1) - a_2 u(n-2)) \qquad (4.25)$$

But $a_1 = 0$, $a_o = 1$ therefore

$$u(n) = b_0 e(n) + b_1 e(n-1) + b_2 e(n-2) - a_2 u(n-2) \qquad (4.26)$$

How ever; a more computer friendly form of discretization is given below.
Proportional Action;

$$\text{Proportional term } P(k) = K_p(\theta(k)_{set} - \theta(k)_{actual}) \qquad (4.27)$$

Where K_p is the proportional gain

Integral Action;

$$\text{Integral Term } I(t) = \frac{K}{T_i} \int_0^t e(t)dt \qquad (4.28)$$

$$\frac{dI}{dt} = \frac{K}{T_i} e(t) \qquad (4.29)$$

The derivative approximated by a forward difference gives;

$$\frac{I(t_{k+1}) - I(t_k)}{h} = \frac{Kh}{T_i} e(t_k) \tag{4.30}$$

This leads to the following recursive equation for the integral term

$$I(t_{k+1}) = I(t_k) + \frac{Kh}{T_i} e(t_k) \tag{4.31}$$

Derivative Action

The derivative term is given by Equation;

$$\frac{T_d}{N} \frac{dD}{dt} + D = -KT_d \frac{d\theta}{dt} \tag{4.32}$$

This equation can be approximated in the same way as the integral term. In this case we approximate the derivatives by a backward difference.

$$\frac{T_d}{N} \frac{D(t_k) - D(t_{k-1})}{h} + D(t_k) = -KT_d \frac{\theta_k - \theta_{k-1}}{h} \tag{4.33}$$

This can be written as

$$D(t_k) = \frac{T_d}{T_d + Nh} D(t_{k-1}) - \frac{KT_d N}{T_d + Nh} (\theta_k - \theta_{k-1}) \tag{4.34}$$

The advantage of using backward difference is that the parameter
$T_d / (T_d + Nh)$ is in the range 0 to 1 for all values of the parameters. This guarantees that the difference equation is stable.

Summarizing we find that the PID controller can be approximated by;

$$e(t_k) = r(t_k) - \theta(t_k) \tag{4.35}$$

$$P(t_k) = k \times et_k \tag{4.36}$$

$$D(t_k) = \frac{T_d}{T_d + Nh} (D(t_{k-1}) - kN(\theta_k - \theta_{k-1})) \tag{4.37}$$

$$U(t_k) = P(t_k) + I(t_k) + D(t_k) \tag{4.38}$$

$$I(t_{k+1}) = I(t_k) + \frac{kh}{T_i} e(t_k) \tag{4.39}$$

4.6.1 Implementation of the Digital Controller

The PID controller is implemented on the PIC16f877 microcontroller. Analog input 1 (pin no:2) is used as the analog input of the sensor input, Port D is used as the digital reference input. However, the analog input produces a 10 bit sensor input but the digital reference input is an eight bit number therefore, in order to make internal calculations easier, 8 bit reference is scaled to represent a 10 bit number. The PID controller is implemented according to the following block diagram.

PIC16f877A program block diagram
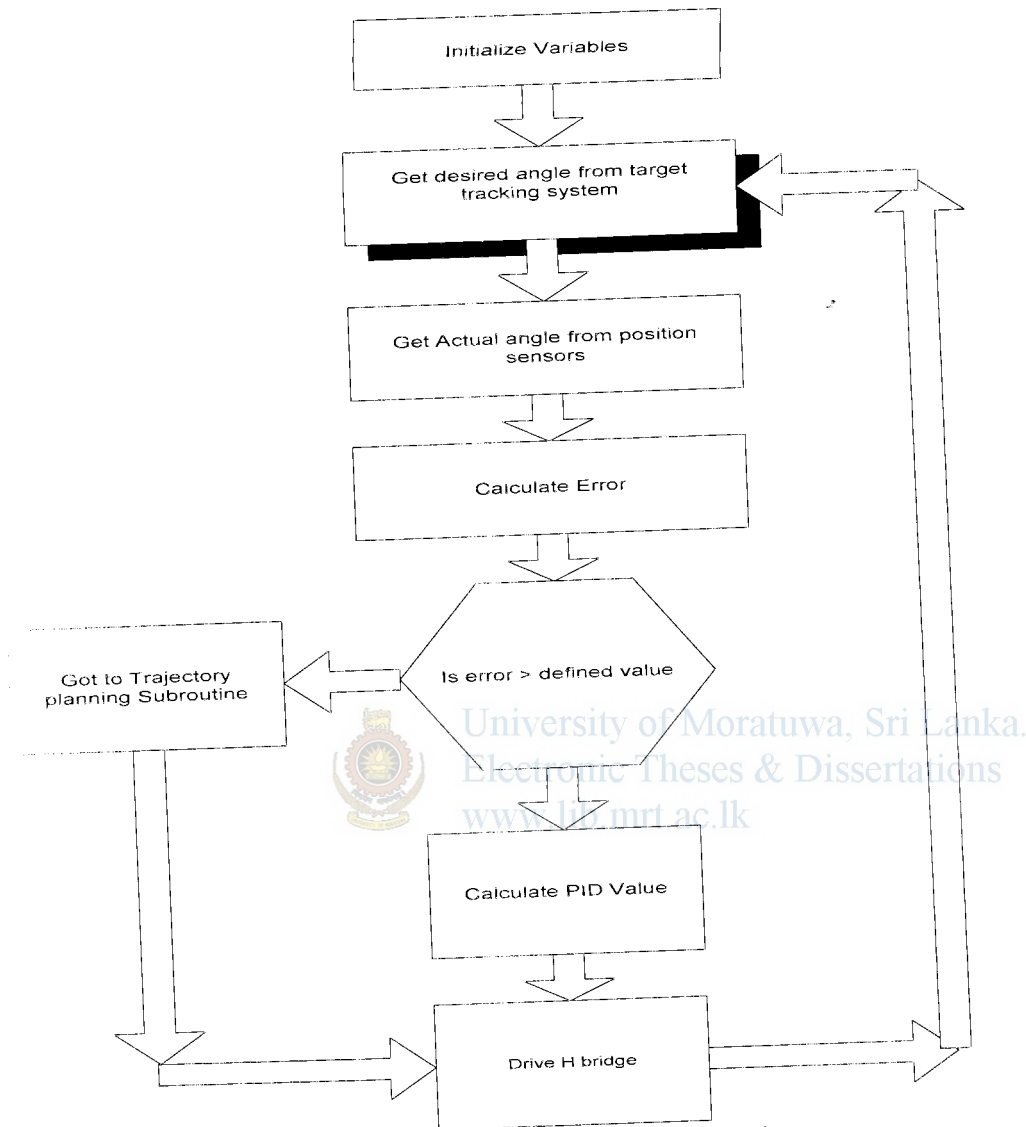
Fig 4.24 block diagram of the PID implementation

Fig4.24: shows the block diagram of the PID implementation see appendix B for completer pic basic pro source code file.

4.7 Trajectory planning

Since the system is for military application, performance is paramount in such applications energy efficiency and aesthetics of the finished product are of lesser priority. Due to the low bandwidth of the system and the high gear ratio, smoothness of movement is anyway assured but the design can over look trajectory planning algorithms as the requirement is to get the target under surveillance as quickly as possible. In this process the I was willing to sacrifice energy efficiency for high performance. Another concern with movements without

trajectory planning is the stress exerted on output stages due to sudden changes in direction. To counter these concerns, electronics are designed with large safety margins.

Results

5.1 Response to external target inputs

To asses the performance of the mechanism, it is made to respond to various inputs generated by an external target simulator. Target inputs are generated by a random number generator and fed to the computer as joint angle parameters.
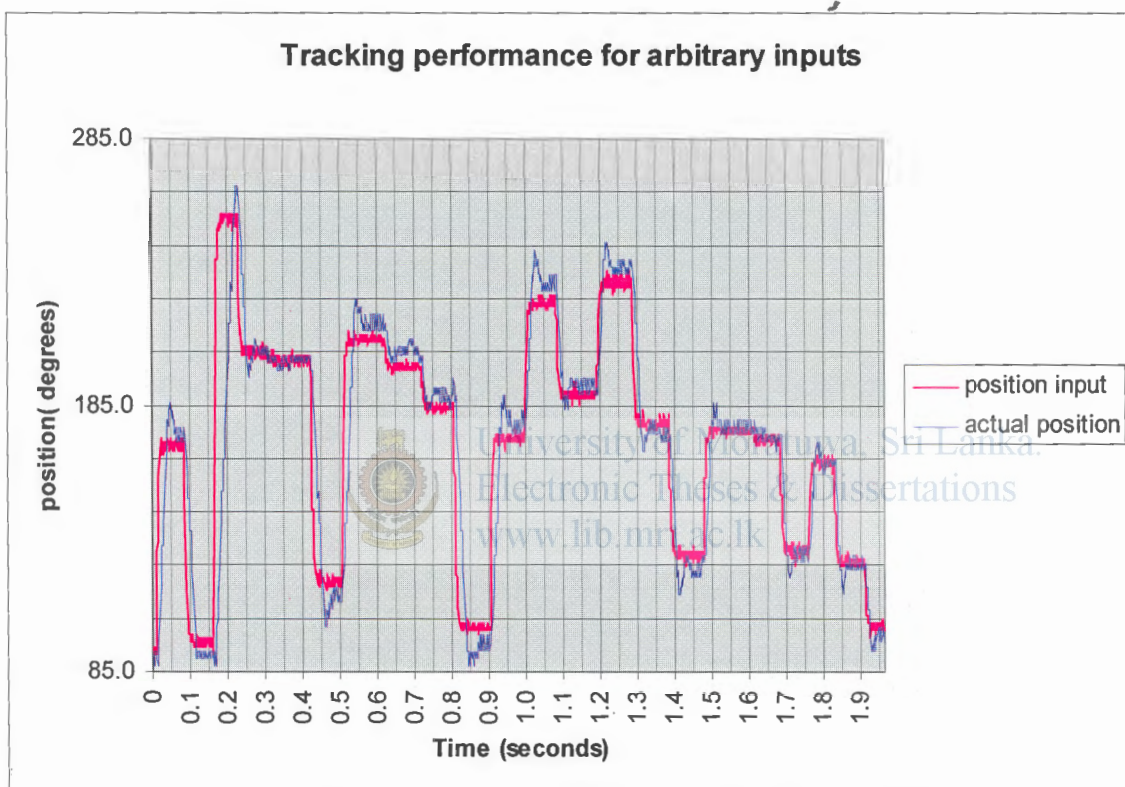
Fig5.1   response to arbitrary external target inputs

Fig5.1   Shows target tracking performance of the pan Mechanism. Channel 4 (Blue trace) is the position input, Channel 3 (purple trace) is the tracking output. As can be seen there is good tracking performance but the mechanism lags the input.

5.2 Response to External Sinusoidal Inputs
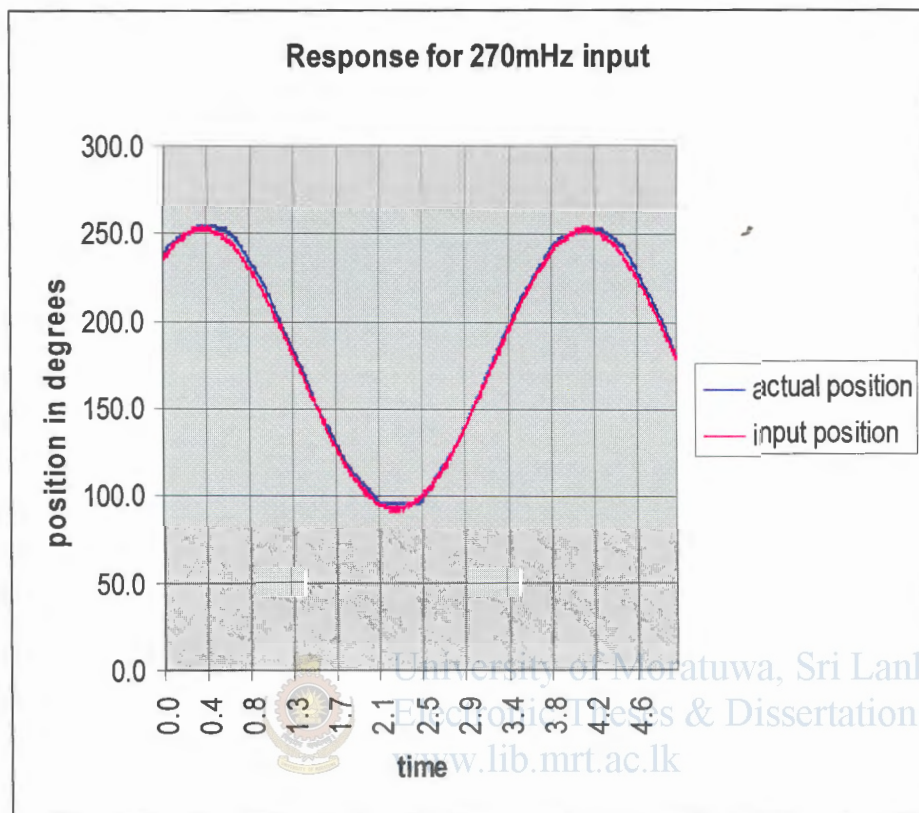
Fig5.2(a): input sinusoidal signal of 270 mHz,

At an input frequency of 270 mHz, the lag is barely noticeable and the position follows the input position input faithfully.
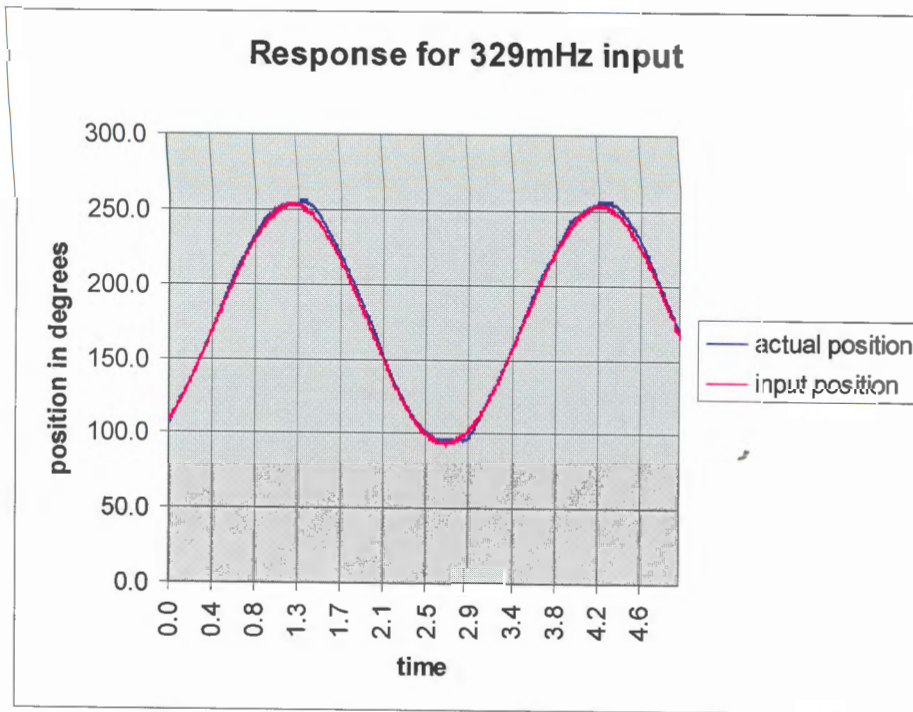
Fig5.2 (b) Input signal of 329 mHz
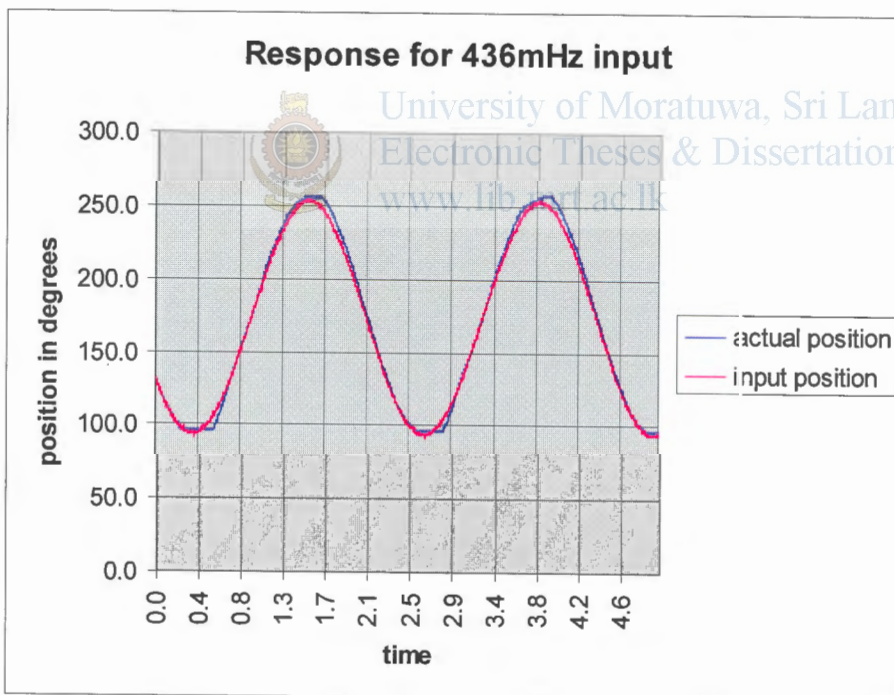
Fig 5.2 (c) Input signal of 436 mHz

When the frequency input is 329 mHz output response is still good but when the input frequency increases to 436 mHz, the lag becomes apparent.
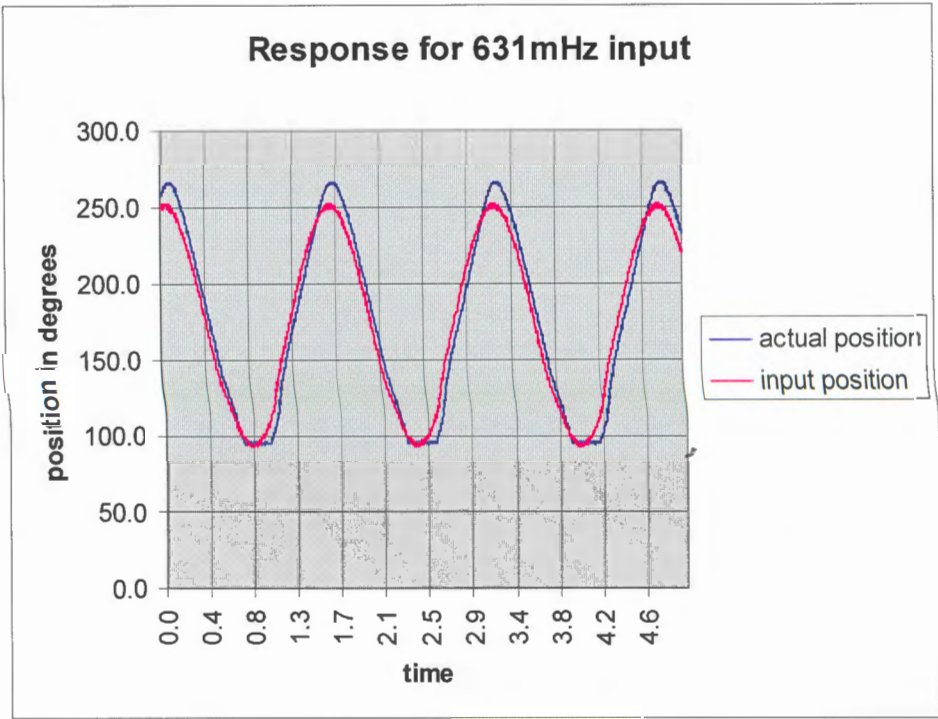
Fig 5.2 (d) Input signal of 631mHz
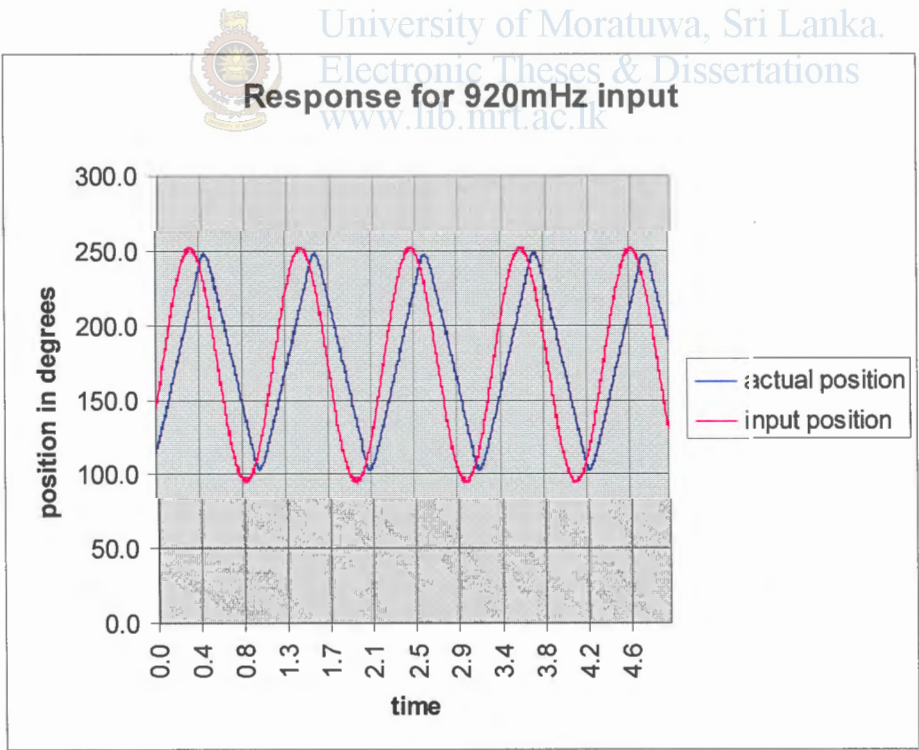
Fig 5.2 (e) Input signal of 920mHz

Above two graphs show the output response to input frequencies of 631mHz and 920mHz, at 631mHz there appears to be a resonance peak, ie: output amplitude is Large than the input amplitude and at 920 mHz time lag is apparent and severe.

Chapter 6

Conclusions and further developments

A vision based target tracking turret base was designed constructed and Laboratory tested. Testing revealed very satisfactory performance of the system. Chapter 5 analyzed the response of the final mechanism to various inputs in detail, As a general rule feedback loop bandwidth should be in the order of 3 to 4 larger than the set point bandwidth. However according to the FFT analysis we consider the set point band width to be in the rage of 1 Hz.

System modeling intentionally disregards non-linear effects such as gravity effects, carioles force, coupling effects etc. While this is reasonable when the system is slow moving and the accuracy of target tracking is less important, they cannot be ignored in a high speed, high accuracy system. A more realistic modeling of the system (Lagrange modeling) needs to carried out for the larger system.

Tracking response is extremely satisfactory at very low frequency levels but as the frequency increases, tracking response gets degraded both in terms of amplitude and delay. Some form of delay is unavoidable as a result of the bandwidth of the system but these shortcomings can be minimized by the use of advanced control systems such as feed forward loops and partitioned PD controllers, which has a servo based section and a model based section in its control architecture. For such systems high speed online calculation of inputs to the drive motors is essential, As such, use of high speed DSP's are needed.

Though, this system uses a vision system to replace the radar system, commercial prototype will have to make use of real inputs from a primary radar system. This is because data from radar system arrive much less frequently and the system will have to make predictions of target position.

By referring to FFT analysis of the target, it can be argued that power at 1 Hz is extremely low, therefore for all practical purposes (except in extreme circumstances) the set point bandwidth (or the target bandwidth) is around 0.3Hz, in which case the available bandwidth is more than sufficient to track target movements. But a detailed study is needed validate this conclusion.

The system is inherently stable with a phase margin of 82deg, which means that the gain can be further increased (actuators permitting) without compromising the stability of the system. Therefore we can design the gun turret so that it is capable of engaging the target at much close range. However, use of higher torque actuators may lead to lower phase margin or even system instability. In which case Phase margin can be adjusted using phase lead compensators.

Throughout the design process of this mechanism I experienced the paralyzing limitations imposed by less than ideal sensors. Therefore any commercialization of the above unit needs highest quality sensors. High resolution absolute rotary sensors are essential for accurate positioning.

On a commercial version, stress analysis needs to be carried out to counter the impact forces due to artillery fire.

Due to sensor noise, imperfections of PWM driver algorithm and target tracking system noise, there is considerable vibration after the target position is achieved. Therefore better sensor outputs needs to be acquired possibly with the use of digital filter such as kalman filtering on both image acquisition systems as well as on the position sensor outputs.

Further development of the model will require significant amounts of money. It will also require access to real data inputs from radar systems, which requires clearance from government agencies such as the ministry of defense. A detailed proposal will be made to the ministry of defense with the intention of obtaining funds for developing a commercial version.

References:

[1] Ser-Nam Lim, Ahmed Elagammal, Larry S Davis, " Image based pan tilt cameral control in a multi camera surveillance environment." University of Maryland, Collage Park, 2002.

[2] Anirbhan Mukurjee, "Design and Digital implementation of a PID controller for a simulated rotory knife cutter", Master Thesis, Youngstown state university ,1998.

[4] Duy Nguyen-Tuong, Jan peters, "Learning Robot Dynamics for Computed Torque Control using Local Gaussian Processes Regression." Max plank institute of biological cybernetics, Spemannstraße 38, 72076 T ubingen, ECSIS Symposium on Learning and Adaptive Behaviors for Robotic Systems."

[5] http://telerobot.mech.uwa.edu.au/ROBOT (University Web)

[6] R. K. Mittal and I. J. Nagrath, "Robotics and Control", New Delhi. Tata McGraw-Hill, 2007.

[7] Benjamin C Kuo, "Automatic control systems", New Delhi, Prentice-Hall. 1995.

[8] Saeed B. Niku, "Introduction to robotics, Analysys, Systems, Applications" , New Delhi, Prentice-Hall,2005.

[9] I. J. Nagrath and M Gopal, "Control systems Engineering", New Delhi, New Age International, 2006.

[10] N.Mohan, T.M. Undeland, W.P. Robins, "Power Electronics, Converters, Applications and Design", New Yourk, John wiley & Sons, Inc,1995

[11] Theodore F. Bogart, Jr, "Electronic Devices and Circuits", New Delhi, Universal book stall, 1994.

[12] John D. Lenk, "Circuit Encyclopedia and Trouble shooting Guide", New York, McGraw Hill, 2000.

[13] Biswa Nath Datta, "Numerical methods for linear control systems", California, Elsivier, 2004.

[14] Seth Hutchinson, Gregory D. Hager, Peter I. Korke, "A Tutorial on Visual Servo Control", IEEE Transactions on Robotics and Automation, Vol 12, No5, October 1996.

Appendix A (Coordinate transformation);
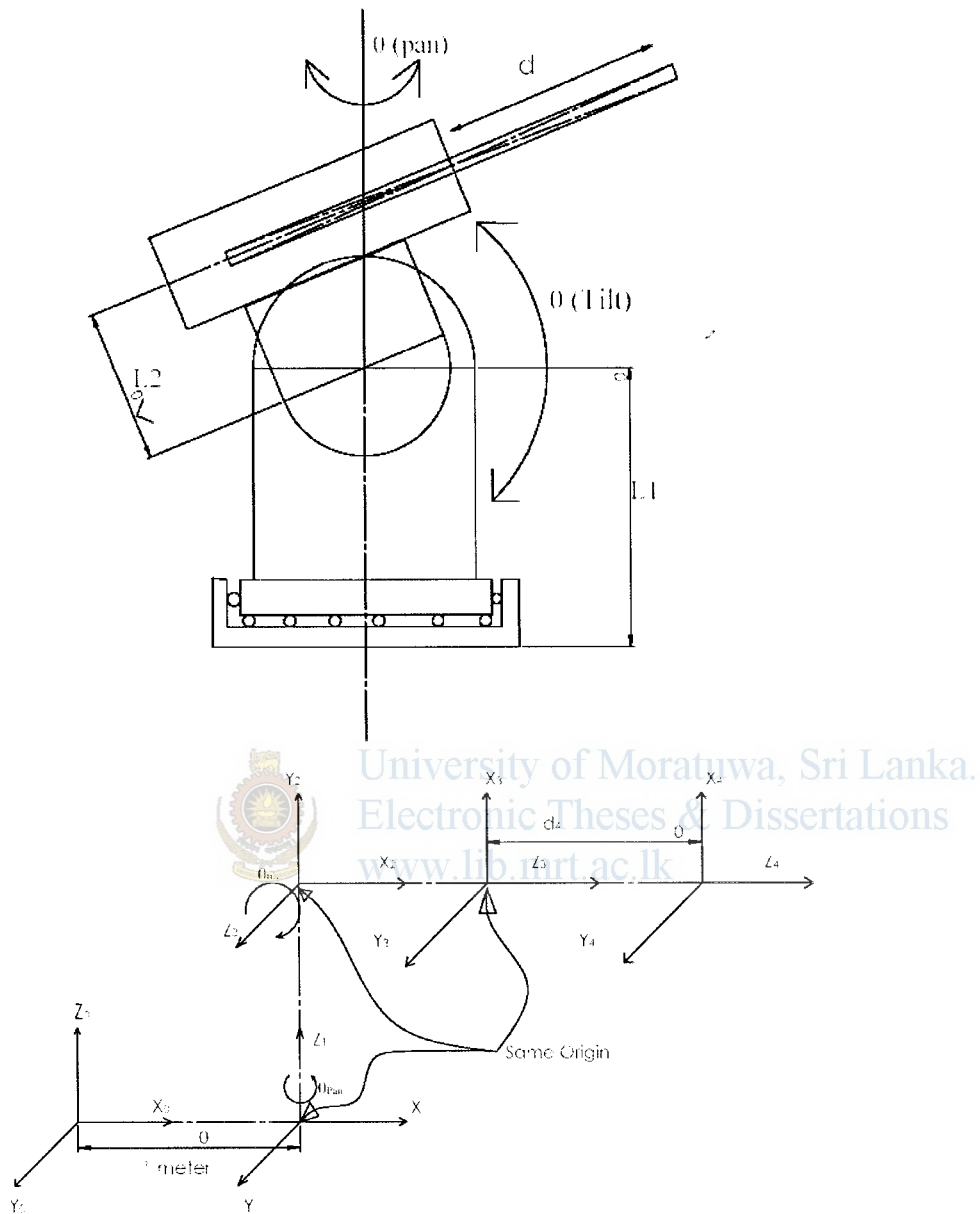
Source: Mittal and Nagrath, "Robotics and Control"

$$\theta_{pan} = \theta_1$$
$$\theta_{tilt} = \theta_2$$

As such the DH table for this robot manipulator is as follows

In case the error is larger than 1 Degree the program needs to branch in to a trajectory pla

$Link_i$	a_i	a_i	d_i	θ_i	q_i
1	1	0^0	0	0	-
2	0	90^0	0	θ_1	θ_1
3	0	-90	0	θ_2	θ_2
4	0	0	d_4	0	d_4

$$^0T_1 = \begin{bmatrix} 1 & 0 & 0 & 1 \\ 0 & 1 & 0 & 0 \\ 0 & 0 & 1 & 0 \\ 0 & 0 & 0 & 1 \end{bmatrix}$$

$$^1T_2 = \begin{bmatrix} C1 & 0 & S1 & 0 \\ S1 & 0 & -C1 & 0 \\ 0 & 1 & 0 & 0 \\ 0 & 0 & 0 & 1 \end{bmatrix}$$

$$^2T_3 = \begin{bmatrix} C2 & 0 & S2 & 0 \\ S2 & 0 & -C2 & 0 \\ 0 & -1 & 0 & 0 \\ 0 & 0 & 0 & 1 \end{bmatrix}$$

$$^3T_4 = \begin{bmatrix} 1 & 0 & 0 & 0 \\ 0 & 1 & 0 & 0 \\ 0 & 0 & 1 & d_4 \\ 0 & 0 & 0 & 1 \end{bmatrix}$$

$$^0T_4 = {}^0T_1 \times {}^1T_2 \times {}^2T_3 \times {}^3T_4$$

$$^0T_4 = \begin{bmatrix} C_1C_2 & -S_1 & -C_1S_2 & -C_1S_2d_4+1 \\ S_1C_2 & C_1 & -S_1S_2 & -S_1S_2d_4 \\ S_2 & 0 & C_2 & C_2d_4 \\ 0 & 0 & 0 & 1 \end{bmatrix} = \begin{bmatrix} r_{11} & r_{12} & r_{13} & r_{14} \\ r_{21} & r_{22} & r_{23} & r_{24} \\ r_{31} & r_{32} & r_{33} & r_{34} \\ r_{41} & r_{42} & r_{43} & r_{44} \end{bmatrix}$$

$$-C_1S_2d_4 = r_{14} - 1$$

$$-S_1S_2d_4 = r_{24}$$

$$d_4C_2 = r_{34}$$

58

$$\theta_1 = \theta_{pan} = A \tan 2 \left(-r_{24}, -(r_{14} - 1) \right) \text{------------------------(2)}$$

$$\theta_2 = \theta_{tilt} = A \tan 2 \left(\pm \sqrt{(r_{14} - 1)^2 + r_{24}^2}, r_{34} \right) \text{-----------------------(3)}$$

$$x = r_{14}$$

$$y = r_{24}$$

$$z = r_{34}$$

Appendix B (PIC basic pro souce code for PID implementation)

```
'************************* E X A M P L E *************************
'***************************************************************
pan_theta VAR WORD              '<---This is my Actual theta(angle)

pan_theta_ref VAR WORD           '<---This is my desired angle


pan_theta_ref_hi_clamp VAR word
pan_theta_ref_low_clamp Var word
pan_Direction var PortC.0
pan_Direction_Last Var bit

adval var word
adval1 var word
pan_pid_Status var byte           'Status of the PID-filter can be read here.
pan_pid_Status_Out_Sat var pan_pid_Status.7    'Flag for saturated output
pan_pid_Status_I_Sat var pan_pid_status.6      'Flag for saturated Integral drive.
pan_pid_Kp Var Word               'Proportional gain.
pan_pid_Ki Var Word               'Integral gain.
pan_pid_Kd Var Word               'Derivative gain.
pan_pid_Error Var Word            'PID Filter input. (setpoint - actual)
pan_pid_Out Var Word              'PID Filter output (P + I + D)
pan_pid_Ti var BYTE               'Time constant for the integral time
pan_pid_I_Clamp var word          'Clamp for the integrator windup.
pan_pid_Out_Clamp var word        'Clamp the final output to value in this var.
Define ADC_BITS 10                        ' Set number of bits in result
'***************************************************************
*****
'**************** PID-Filter "internal" variables *************************
'***************************************************************
*****
pan_pid_P Var Word             'Proportional drive.
pan_pid_I VAR Word              'Integral drive.
pan_pid_D Var Word             'Derivative drive.
pan_pid_Sign Var BIT              'Keeps track of the sign of various values
pan_pid_LastError var word        'Last error, used for calculating D drive
pan_pid_Ei Var Word            'Integral drive accumulator.
pan_pid_IntCount Var Byte         'Counter for the integrator, matches against Ti


'***************************************************************
*****
'**************** Initialise variables *************************
'***************************************************************
*****
pan_pid_P = 0                  'Reset P, I & D variables.
pan_pid_I = 0
pan_pid_D = 0
```

60

```
ADCON1 = %10000000 ' Set PORTA analog and right justify result
'****************************************************************
'These variables are declared by the incPID routine but
'the user needs to assign values to them.
'Gosub GetAD2
  pan_pid_Kp = %1010111100 'Set Kp to 7.0 original 256
  pan_pid_Ki=%10                  'Set Ki to 0.5
          pan_pid_Kd = %11001000              'Set Kd to 2.14 original 128
  pan_pid_Ti = %11                'Update I-term every 3rd call to PID
  pan_pid_I_Clamp = %1100100           'Clamp I-term to max ±100
  pan_pid_Out_Clamp =%11111111         'Clamp the final output to ±511
          pan_theta_ref_hi_clamp = %1100100000
pan_theta_ref_low_clamp =%110010
          TRISC = 0


Start:

  Gosub GetAD_pan                'Get position from A to D
          pan_pid_Error = pan_theta_ref - pan_theta    'Calculate the error
  Gosub PID_pan                              'Result returned in piddrive
  pan_Direction = pan_pid_Out.15
          if pan_Direction <> pan_Direction_Last and pan_pid_Out > 0 Then
          pan_Direction_Last = pan_Direction
          endif
                                             'Set  direction  pin
accordning to sign

          'pan_pid_Out = ABS pan_pid_Out                          'Convert
from two's comp. to absolute

          If pan_Direction_Last then
          HPWM 2, 255, 250
          HPWM 1, pan_pid_Out , 250
          HPWM 2, 255, 250                      'Set PWM output
          Else

          pan_pid_Out = -pan_pid_Out
          HPWM 1, 255, 250
  HPWM 2, pan_pid_Out , 250

          endif

          ADRESH = 0
          ADRESL = 0
          adval.highbyte = 0
          adval.lowbyte = 0
          adval = 0
          adval1.highbyte = 0
          adval1.highbyte = 0
          adval1 = 0
```

```
'Pauseus 1                                          'Wait.... original 10

          pan_Direction_Last = pan_Direction
          Goto Start
               '...and do it again.


'*******************************************************************************
*******
PID_pan:                        'This is the entrypoint from the main app.
'*******************************************************************************
*****
'********************** P I D   F I L T E R  ***********************************
'*******************************************************************************
*****

'Calculate the proportional drive


pan_pid_P = (ABS pan_pid_Error) */ pan_pid_Kp    'Multiply by the P-gain
If pan_pid_Error.15 then pan_pid_P = -pan_pid_P   'Re-apply sign if pan_pid_Error is neg
'*******************************************************************************
*****
'*******************************************************************************
*****
'Calculate the Integral drive
pan_pid_Ei = pan_pid_Ei + pan_pid_Error       'Add error to acumulator.
pan_pid_IntCount = pan_pid_IntCount + 1        'Increment the reset-time counter.
If pan_pid_IntCount >= pan_pid_Ti then         'Is it time to update the I-term?
  pan_pid_Sign = pan_pid_Ei.15            'Save Sign
  pan_pid_Ei = ABS pan_pid_Ei            'Work with positive numbers
  pan_pid_Ei = pan_pid_Ei */ pan_pid_Ki      'Multiply by Ki gain
  pan_pid_Ei = pan_pid_Ei / pan_pid_Ti       'Divide by the reset time
  If pan_pid_Sign then pan_pid_Ei = -pan_pid_Ei  'Re-apply sign
  pan_pid_I = pan_pid_I + pan_pid_Ei         'Update I drive
  pan_pid_Sign = pan_pid_I.15            'Save Sign
  pan_pid_I = ABS pan_pid_I             'Work with positive numbers
  if pan_pid_I >= pan_pid_I_Clamp then      'I-term is saturated....
    pan_pid_Status_I_Sat = 1          'set pan_pid_I_Clamp flag....
    pan_pid_I = pan_pid_I_Clamp         'and clamp I-terms to what user have set.
  Endif
  If pan_pid_Sign then pan_pid_I = -pan_pid_I    'Re-apply sign
  pan_pid_IntCount = 0             'Reset the counter.
  pan_pid_Ei = 0                'Reset the accumulator.
Endif
'*******************************************************************************
*****
'*******************************************************************************
*****
'Calculate the derivative drive
```

```
    pan_pid_D = pan_pid_Error - pan_pid_LastError
    pan_pid_Sign = pan_pid_D.15              'Save Sign
    pan_pid_D = (ABS pan_pid_D) */ pan_pid_Kd      'Multiply by Kd gain
    If pan_pid_Sign then pan_pid_D = -pan_pid_D      'Re-apply sign.
DerivDone1:
      pan_pid_LastError = pan_pid_Error      'Store error for next D calc.


'****************************************************************
*****
'****************************************************************
*****
'Calculate the total drive.
pan_pid_Out = pan_pid_P + pan_pid_I + pan_pid_D       'Calculate total drive....
pan_pid_Sign = pan_pid_Out.15             'Save Sign
pan_pid_Out = ABS pan_pid_Out                'Convert from two's comp. to abs.
If pan_pid_Out >= pan_pid_Out_Clamp then       'Output is saturated...
   pan_pid_Status_Out_Sat = 1           'set status bit and...
   pan_pid_out = pan_pid_Out_Clamp           'clamp output.
Endif
If pan_pid_Sign then pan_pid_out = -pan_pid_out     'Re-apply sign.
RETURN
```
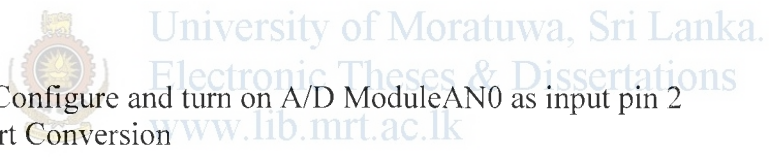
```
GetAD_pan:
ADCON0 = %11000001    'Configure and turn on A/D ModuleAN0 as input pin 2
loop3: ADCON0.2 = 1  ' Start Conversion
notdone3: Pauseus 1
If ADCON0.2 = 1 Then notdone3 ' Wait for low on bit-2 of ADCON0, conversion finished
adval.highbyte = ADRESH ' Move HIGH byte of result to adval
adval.lowbyte = ADRESL ' Move LOW byte of result to adval
adval = adval
pan_theta = adval




pan_theta_ref = portd  * %110           'Make the 8 bit number to 10 bit number, minimum
decimal value is 254 maxis 1019.
            if pan_theta_ref >= pan_theta_ref_hi_clamp then ' Hi
   pan_theta_ref = pan_theta_ref_hi_clamp
else
            if pan_theta_ref <= pan_theta_ref_low_clamp then
            pan_theta_ref = pan_theta_ref_low_clamp
   endif
   endif

Return:

'GetRef_pan
```

Appendix C (.m file for FFT analysis)

```matlab
t = 0:0.0001:5;
A=-0.043296;
B=3.0618;
C=2.0361;
D=-0.20488;
E=0.0073960;
for j = 1 : length(t)
y(1,j)=A+B*t(1,j)+C*t(1,j)^2+D*t(1,j)^3+E*t(1,j)^4;
end
plot (t,y);
title('variation of distance with time (A-10 thunderbolt)');
ylabel('distance (m)');
xlabel('time (s)');

figure
for j =1:length(t)
v(1,j)= B+2*C*t(1,j)+3*D*t(1,j)^2+4*E*t(1,j)^3;
end

for j =1:length(t)
a(1,j)= 2*C+6*D*t(1,j)+12*E*t(1,j)^2;
end

sintheta(1,1) = 5/sqrt(50);
for k=2:length(y)
    sintheta(1,k) =5/sqrt(25+(5-y(1,k))^2);
end
theta = ((asin(sintheta)).*360)/(2*pi);
for n = 2:length(y)-1
   if theta(1,n+1)<theta(1,n)
      theta(1,n+1) = 180 - theta(1,n+1);
   else
      theta(1,n+1) = theta(1,n+1);
   end
end

plot(t,theta);
title('variation of theta with time');
ylabel('angle in degrees');
xlabel('time in seconds');


Fs = 10000;

figure
plot(t,theta)
title('angular variation profile of an A-10 thunder bolt observed from a distance of
300m perpendicular to the path');
```

```
figure
% Use next highest power of 2 greater than or equal to length(x) to calculate FFT.
nfft= 2^(nextpow2(length(theta)));
% Take fft, padding with zeros so that length(fftx) is equal to nfft
fftx = fft(y,nfft);
% Calculate the numberof unique points
NumUniquePts = ceil((nfft+1)/2);
% FFT is symmetric, throw away second half
fftx = fftx(1:NumUniquePts);
% Take the magnitude of fft of x and scale the fft so that it is not a function of % the
length of x
mx = abs(fftx)/length(theta);
% Take the square of the magnitude of fft of x.
mx = mx.^2;

% Since we dropped half the FFT, we multiply mx by 2 to keep the same energy.
% The DC component and Nyquist component, if it exists, are unique and should not
% be mulitplied by 2.
if rem(nfft, 2) % odd nfft excludes Nyquist point
  mx(2:end) = mx(2:end)*2;
else
  mx(2:end -1) = mx(2:end -1)*2;
end
% This is an evenly spaced frequency vector with NumUniquePts points.
f = (0:NumUniquePts-1)*Fs/nfft;
% Generate the plot, title and labels.
plot(f,mx);
title('Power Spectrum of A-10 thunder bolt (angular variation) observed from 3000m');
xlabel('Frequency (Hz)');
ylabel('Power');
AXIS([0 1.5 0 400]);
```

Appendix D (.m file for transfer function extraction from simulink model)

%get the state space model of the simulink modelpantiltmodel

```
[A,B,C,D] = linmod('pantiltmodel1')
 %do the state space to tf transformation
[numcl,dencl] = ss2tf(A,B,C,D);
%observe the step response
step(numcl,dencl);
Grid Minor
figure;
bode(numcl,dencl);
 % Velocity transfer function
Gv = tf(numcl,dencl)
 %define the transfer function of s
s = tf([1 0],1);
 % position(angle) transfer function
Ga = Gv/s
Gv.inputName = 'Voltage';
Gv.OutputName = 'velocity';
Ga.InputName = 'Voltage';
Ga.OutputName = 'Angle';
figure;
step(Gv);
Grid Minor
figure;
bode(Gv);
Grid Minor
figure;
step(Ga);
Grid minor
figure;
bode(Ga);
Grid Minor
```

Appendix E (VB scrip program for roborealm)

```
if GetVariable("COG_X")= false then
Set Variable "cogx", GetVariable("cogx_last")
SetVariable "cogx", (GetVariable("COG_X")-
GetVariable("IMAGE_WIDTH")/2)
SetVariable "cogx_last", GetVariable("cogx")
end if
if GetVariable("COG_Y") = false then
SetVariable "cogy", GetVariable("cogy_last")
else
SetVariable "cogy", (GetVariable("COG_Y")-
GetVariable("IMAGE_HEIGHT")/2)
SetVariable "cogy_last", GetVariable("cogy")
end if
```

> If current image loses tracking resort to COG values of previous frame Else calculate COG coordinates with respect to Center of image

```
SetVariable "cogx2", FormatNumber(GetVariable("cogx")*1.1, 1)
SetVariable "cogy2", FormatNumber(GetVariable("cogy")*0.5,1)
SetVariable "angle", FormatNumber(atan2(GetVariable("cogx2"), -150),1)*57
SetVariable "test",
sqrt(Clng(GetVariable("cogx2")*GetVariable("cogx2"))+sqr(150))
SetVariable "angle_tilt", FormatNumber(atan2(GetVariable("cogy"), -
sqrt(Clng(GetVariable("cogx2")*GetVariable("cogx2"))+sqr(150))),1)*57
```

> Convert COG coordinates obtained in pixel values to real values

```
if GetVariable("angle") < 0 then
SetVariable "angle2", 360 - Abs(GetVariable("angle"))
else
SetVariable "angle2", GetVariable("angle")
end if
if GetVariable ("angle2") < 90 then
SetVariable "angle2"  =  90
elseif GetVariable ("angle2") > 270 then
SetVariable "angle2" = 270
end if
```

> Avoid negative values and set upper and lower limits for pan angle

```
if GetVariable("angle_tilt") <0 then
SetVariable "angle_tilt_2", 360 - Abs(GetVariable("angle_tilt"))
Else
SetVariable "angle_tilt_2", GetVariable("angle_tilt")
end if
```

Avoid negative values and set upper and lower limits for pan angle

```
SetVariable "angle_serial1", Cint(255-  (GetVariable("angle2")/180*255-127.5))
SetVariable "angle_tilt_serial1", (Cint((GetVariable("angle_tilt_2")/360)*255))
SetVariable "angle_serial" , GetVariable("angle_serial1")+300
SetVariable "angle_tilt_serial", GetVariable("angle_tilt_serial1")+300
```

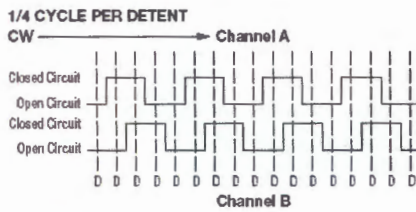Format in suitable form to be transmitted over Rs 232

Appendix F (Quadrature Encoder)
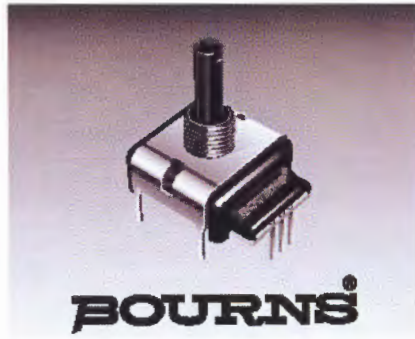
QUADRATURE OUTPUT TABLE
This table is intended to show available outputs as currently defined.
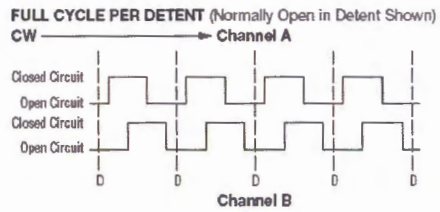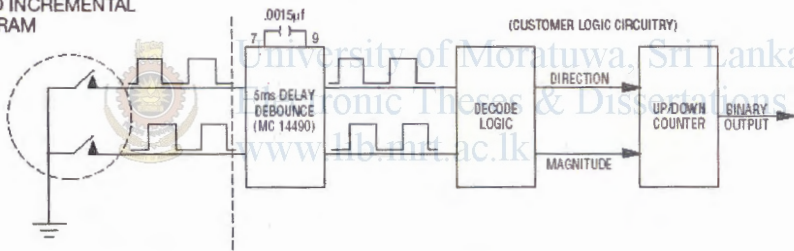
Quadrature Encoder (Courtesy bourns Electronics)

Appendix G (simple potentiometers)

| Single turn potentiometer 10k (Courtesy pankaj potentiometers) | multi turn potentiometer 10k (Courtesy bourns electronics) |

Appendix H (Absolute analog encoders contact less type)

Absolute Analogue Servo Encoder (A^2SE) type NCP-307 (courtesy pankaj potentiometers)

Appendix I

Single Turn Wire Wound Servo Potentiometers, type SS50(courtesy pankaj potentiometers)